Journal of Integer Sequences, Vol. 9 (2006),
Article 06.3.4

On the Farey Fractions with Denominators in Arithmetic Progression

C. Cobeli[1] and A. Zaharescu[2]
Institute of Mathematics of the Romanian Academy
P. O. Box 1-764
Bucharest 70700
Romania
cristian.cobeli@imar.ro
zaharesc@math.uiuc.edu

Abstract

Let $\mathfrak{F}^Q$ be the set of Farey fractions of order Q. Given the integers $\mathfrak{d} \geq 2$ and $0 \leq \mathfrak{c} \leq \mathfrak{d}-1$, let $\mathfrak{F}^Q(\mathfrak{c},\mathfrak{d})$ be the subset of $\mathfrak{F}^Q$ of those fractions whose denominators are $\equiv \mathfrak{c} \pmod{\mathfrak{d}}$, arranged in ascending order. The problem we address here is to show that as $Q \to \infty$, there exists a limit probability measuring the distribution of s-tuples of consecutive denominators of fractions in $\mathfrak{F}^Q(\mathfrak{c},\mathfrak{d})$. This shows that the clusters of points $(q_0/Q, q_1/Q, \ldots, q_s/Q) \in [0,1]^{s+1}$, where $q_0, q_1, \ldots, q_s$ are consecutive denominators of members of $\mathfrak{F}^Q$ produce a limit set, denoted by $\mathcal{D}(\mathfrak{c},\mathfrak{d})$. The shape and the structure of this set are presented in several particular cases.

1 Introduction

Farey fractions have many applications in various areas of mathematics. Recently, they have been successfuly used in some problems on billiards [3, 4] and the two dimensional Lorentz gas [5]. The present paper is a continuation of a series of papers dedicated to the study of the distribution of neighbor denominators of Farey fractions whose denominators are in arithmetic progression. Previously [10, 11, 13, 14] different authors have treated the cases of pairs of odd and even denominators, respectively, while here we deal with tuples of consecutive denominators of fractions in $\mathfrak{F}^Q(\mathfrak{c},\mathfrak{d})$, the set of Farey fractions with

[1]C. Cobeli is partially supported by the CERES Programme of the Romanian Ministry of Education and Research, contract 4-147/2004.

[2]Author's current address: Department of Mathematics, University of Illinois at Urbana-Champaign, Altgeld Hall, 1409 W. Green Street, Urbana, IL, 61801, USA.

denominators $\equiv \mathfrak{c} \pmod{\mathfrak{d}}$. (Here $\mathfrak{c}, \mathfrak{d}$ are integers, with $\mathfrak{d} \geq 2$ and $0 \leq \mathfrak{c} \leq \mathfrak{d} - 1$.) The motivation for their study [1, 3, 4, 6, 7, 8, 9] comes from their role played in different problems of various complexities, varying from applications in the theory of billiards to questions concerned with the zeros of Dirichlet L-functions. Although the present work is mostly self-contained, the reader may refer to the authors [11] and the references within for a wider introduction of the context and the treatment of some calculations.

Two generic neighbor fractions from $\mathfrak{F}^Q$, the set of Farey fractions of order Q, say a'/q' and a''/q'', have two intrinsic properties. Firstly, the sum $q' + q''$ is always greater than Q and secondly, $a''q' - a'q'' = 1$. None of these two properties is generally true for consecutive members of $\mathfrak{F}^Q(\mathfrak{c}, \mathfrak{d})$, but we shall see that they may be recovered as initial instances of some more complex connections.

Given a positive integer $s \geq 1$, our main interest lies on the set of tuples of neighbor denominators of fractions in $\mathfrak{F}^Q(\mathfrak{c}, \mathfrak{d})$:

$$\mathcal{D}_s^Q(\mathfrak{c}, \mathfrak{d}) := \left\{ (q^0, q^1, \ldots, q^s) \colon \begin{array}{l} q^0, q^1, \ldots, q^s \text{ are denominators of} \\ \text{consecutive fractions in } \mathfrak{F}^Q(\mathfrak{c}, \mathfrak{d}) \end{array} \right\}.$$

(Notice that due to some technical constraints, in our notations, the dimension is $s+1$ and not s.) In fact our aim is to show that there is a limiting set $\mathcal{D}_s(\mathfrak{c}, \mathfrak{d})$ of the scaled set of points $\mathcal{D}_s^Q(\mathfrak{c}, \mathfrak{d})/Q \subset [0,1]^{s+1}$, as $Q \to \infty$. Strictly speaking, this is the set of limit points of sequences $\{\mathbf{x}_Q\}_{Q \geq 2}$, where each $\mathbf{x}_Q$ is picked from $\mathcal{D}_s^Q(\mathfrak{c}, \mathfrak{d})/Q$.

More in depth information on $\mathcal{D}_s(\mathfrak{c}, \mathfrak{d})$ is revealed if one knows the concentration of points across its expanse. The answer is given by Theorem 2 below, which shows that there exists a local density function on $\mathcal{D}_s(\mathfrak{c}, \mathfrak{d})$ and gives an explicit expression for it. Next, let us see the formal definition. Let $\mathbf{x} = (x_0, \ldots, x_s)$ be a generic point in $[0,1]^{s+1}$ and denote by $g_s(\mathbf{x}) = g_s(\mathbf{x}; \mathfrak{c}, \mathfrak{d})$ the function that gives the local density of points $(q_0/Q, q_1/Q, \ldots, q_s/Q)$ in the $s+1$-dimensional unit cube, as $Q \to \infty$, where $q_0, q_1, \ldots, q_s$ are consecutive denominators of fractions in $\mathfrak{F}^Q(\mathfrak{c}, \mathfrak{d})$. At any point $\mathbf{u} = (u_0, \ldots, u_s) \in [0,1]^{s+1}$, we define $g_s(\mathbf{u})$ by

$$g_s(\mathbf{u}) := \lim_{\eta \to 0} \frac{\lim\limits_{Q \to \infty} \frac{\#\left(\square \cap \mathcal{D}_s^Q(\mathfrak{c}, \mathfrak{d})/Q\right)}{\#\mathcal{D}_s^Q(\mathfrak{c}, \mathfrak{d})}}{4\eta^2}, \tag{1}$$

where $\square \subset \mathbb{R}^{s+1}$ are cubes of edge 2η centered at $\mathbf{u}$.

The fact that any sequence of consecutive denominators in $\mathfrak{F}^Q$ is uniquely determined by its first two terms has important consequences. Here we are interested in the shape of $\mathcal{D}_s(\mathfrak{c}, \mathfrak{d})$. It turns out that the framework of $\mathcal{D}_s(\mathfrak{c}, \mathfrak{d})$ is built by a union of two dimensional compact surfaces in $\mathbb{R}^{s+1}$. This is the reason for which we have divided in the right-hand side of (1) by the area of a square of edge 2η only, and not by $(2\eta)^{s+1}$.

Thus, basically, $g_s(\mathbf{u}) = g_s(u, v)$ is a function of two variables. Here (u, v) will run over a domain that embodies the Farey series, namely the Farey triangle with vertices $(0,1)$; $(1,0)$; $(1,1)$, denoted by $\mathcal{T}$.

Suppose now that $s = 1$, that is, we are in dimension two. We conclude this introduction with some remarks on the shape of $\mathcal{D}_1(\mathfrak{c}, \mathfrak{d})$, for different $\mathfrak{c}$ and $\mathfrak{d}$ that we have tested (see details, tables and pictures in Section 11). It is likely that our observations extend over all $\mathfrak{c}$ and $\mathfrak{d} \geq 2$.

The first thing to be remarked is the fact that for any $\mathfrak{d} \geq 2$, $\mathcal{D}_1(\mathfrak{c}, \mathfrak{d})$ is a polygon obtained as a union of some sequences of polygonal sets with constant local density on each of them. Moreover, one of these polygons is large enough to include all the others. But the most noteworthy property is that each of these constant-density-polygons has a vertex at $(1, 1)$ and looks like a mosaic composed by polygonal pieces, most of them being quadrangles. The fact that the mosaics exist is not just an accidental occurrence; on the contrary, more and more pieces fit into mosaics with a larger and larger number of components as $\mathfrak{d}$ increases. The mosaics are either symmetric with respect to the first diagonal or they appear in pairs, whose components are symmetric to each other with respect to the first diagonal.

It is not true, as one would guess from tests with many acceptably small $\mathfrak{d}$'s and different $\mathfrak{c}$'s, that the larger mosaic (most likely equal to $\mathcal{D}_1(\mathfrak{c}, \mathfrak{d})$) is always a quadrangle. The first counter-example is $\mathcal{D}_1(3, 12)$, which is a hexagon (see Fig. 13). The shape of the mosaics is more regular when $\mathfrak{d}$ has fewer prime factors. In particular, for each prime modulus $\mathfrak{d}$, the exterior frame of all the mosaics is the same with that from the case $\mathfrak{d} = 2$, $\mathfrak{c} = 0$ (cf. [11, Fig. 5, 6]), which in turn was the same in the case $\mathfrak{d} = 2$, $\mathfrak{c} = 1$ (cf. [10, Fig. 2]). Mosaics having exactly the same form appear in other cases, too. For example, this happens when $\mathfrak{d} = 4$, $\mathfrak{c} = 0$, and the event has another interesting feature: each of the mentioned mosaics appear twice. As opposed to the prime modulus instance, we have included in Section 11 the pictures that appear in the case $\mathfrak{d} = 12$, $\mathfrak{c} = 3$. One may appreciate these mosaics for their proportions, unexpected shape and beauty.

2 Notations and Prerequisites

Suppose the integer Q is sufficiently large, but fixed. We also fix $\mathfrak{d} \geq 2$, the modulus, $0 \leq \mathfrak{c} \leq \mathfrak{d} - 1$, the residue class, and an integer $s \geq 1$ ($s + 1$ is the dimension).

Then, we define recursively the following objects. For $0 < x, y \leq 1$, let $x_j^{\mathcal{L}}(x, y) = x_j^{\mathcal{L}}$ be given by $x_{-1}^{\mathcal{L}} = x$, $x_0^{\mathcal{L}} = y$ and $x_j^{\mathcal{L}} = k_j x_{j-1}^{\mathcal{L}} - x_{j-2}^{\mathcal{L}}$, for $j \geq 1$, where $k_j = k_j(x, y) := \left[\frac{1 + x_{j-2}^{\mathcal{L}}}{x_{j-1}^{\mathcal{L}}}\right]$. We say that x, y are *generators* of $\mathbf{x}^{\mathcal{L}}$, and of $\mathbf{k}$ also, or that $\mathbf{x}^{\mathcal{L}}$ and $\mathbf{k}$ are *generated* by x, y. (We use bold fonts to denote vectors with components indicated by the same letters in normal font and subscripts belonging to ranges that become clear from the context.)

In order to get a sequence of consecutive denominators of fractions in $\mathfrak{F}^Q$, it suffices to know only the first two of them. Moreover, any two coprime integers $1 \leq q', q'' \leq Q$, with $q' + q'' > Q$, appear exactly once in the sequence of consecutive denominators of fractions in $\mathfrak{F}^Q$. Then the subsequent denominators are obtained as follows. Given two neighbor denominators $1 \leq q', q'' \leq Q$, they are succeeded by $q_1^{\mathcal{L}}, q_2^{\mathcal{L}}, \ldots$, where $q_j^{\mathcal{L}}(q', q'') = q_j^{\mathcal{L}} := k_j q_{j-1}^{\mathcal{L}} - q_{j-2}^{\mathcal{L}}$, for $j \geq 1$, and $k_j = k_j(q', q'') = \left[\frac{Q + q_{j-2}^{\mathcal{L}}}{q_{j-1}^{\mathcal{L}}}\right]$. We put $q_{-1}^{\mathcal{L}} = q'$, $q_0^{\mathcal{L}} = q''$. Notice that these values of k_j coincide with those defined above if $x = q'/Q$ and $y = q''/Q$. Then, in order to simplify the notation, we write $\mathbf{k}(q', q'')$ instead of $\mathbf{k}(q'/Q, q''/Q)$. As before, we say that q', q'' are *generators* of $\mathbf{q}^{\mathcal{L}}$ and of $\mathbf{k}$ or that $\mathbf{q}^{\mathcal{L}}$ and $\mathbf{k}$ are *generated* by q', q''.

A good way to look at a tuple $\mathbf{k} = (k_1, \ldots, k_n)$ is to think that it is associated with the whole $(n+2)$-tuple $\mathbf{q} = (q', q'', q_1, \ldots, q_n)$ of consecutive denominators in $\mathfrak{F}^Q$. We remark that the link between $\mathbf{k}$ and $\mathbf{q}$ is also made by the relations: $k_1 = (q' + q_1)/q''$, $k_2 = (q'' + q_2)/q_1$,

$k_3 = (q_1 + q_3)/q_2$, $k_4 = (q_2 + q_4)/q_3$, etc.

It is plain that $k_j \geq 1$ for $j \geq 1$. In the extreme case $n = 0$, the vector $\mathbf{k}$ is empty (that is, it has no components) because there is no mediant between consecutive denominators. In this case we say that $\mathbf{k}$ has order zero.

In general, consecutive fractions in $\mathfrak{F}^Q(\mathfrak{c}, \mathfrak{d})$ are not necessarily consecutive in $\mathfrak{F}^Q$, but have intercalated in-between several other fractions from $\mathfrak{F}^Q$. We remark also that many consecutive denominators of fractions in $\mathfrak{F}^Q(\mathfrak{c}, \mathfrak{d})$ are not necessarily coprime. Let $\mathbf{r} = (r_1, \ldots, r_s)$ be an s-tuple of positive integers, and denote $|\mathbf{r}| = r_1 + \cdots + r_s$. We say that $\mathbf{q} = (q_0, \ldots, q_s)$, a tuple of consecutive denominators of fractions in $\mathfrak{F}^Q(\mathfrak{c}, \mathfrak{d})$, is *of type* $\mathtt{T}(\mathbf{r})$, if $\mathbf{q} \equiv \mathfrak{c} \pmod{\mathfrak{d}}$[3] and there exists a pair of consecutive denominators (q', q'') in $\mathfrak{F}^Q$ with $q^{\mathcal{L}}_{-1}(q', q'') = q_0$, $q^{\mathcal{L}}_{-1+r_1}(q', q'') = q_1, \ldots, q^{\mathcal{L}}_{-1+r_1+\cdots+r_s}(q', q'') = q_s$, and $q^{\mathcal{L}}_j(q', q'') \not\equiv \mathfrak{c} \pmod{\mathfrak{d}}$, for $j \in \{0, \ldots, |\mathbf{r}| - 1\} \setminus \{r_1 - 1, \ldots, r_1 + \cdots + r_s - 1\}$. In this case we also say that the tuple $\mathbf{k}(q', q''; |\mathbf{r}| - 1) = (k_1, \ldots, k_{|\mathbf{r}|-1})$, with $k_j = k_j(q', q'')$ is *of type* $\mathtt{T}(\mathbf{r})$. To select the components that are $\equiv \mathfrak{c} \pmod{\mathfrak{d}}$, we define the *choice application* $F^Q_{\mathbf{r}} \colon \mathbb{N}^2 \to \mathbb{N}^{s+1}$, with

$$F^Q_{\mathbf{r}}(q', q'') := \left(q^{\mathcal{L}}_{-1}, q^{\mathcal{L}}_{-1+r_1}, \ldots, q^{\mathcal{L}}_{-1+r_1+\cdots+r_s}\right).$$

Similarly, for $x, y \in (0, 1]$, with $x + y > 1$, we also put

$$F_{\mathbf{r}}(x, y) := \left(x^{\mathcal{L}}_{-1}, x^{\mathcal{L}}_{-1+r_1}, \ldots, x^{\mathcal{L}}_{-1+r_1+\cdots+r_s}\right).$$

Let $\mathcal{A}_{\mathbf{r}}(\mathfrak{c}, \mathfrak{d})$ be the set of all $\mathbf{k}(q', q''; |\mathbf{r}| - 1)$ of type $\mathtt{T}(\mathbf{r})$, for any q', q''. We remark that the generators of such a $\mathbf{k}$ are, in general, not unique. Then, for any $\mathbf{k} \in \mathcal{A}_{\mathbf{r}}(\mathfrak{c}, \mathfrak{d})$, we consider the set of residues relatively prime to $\mathfrak{c}$, given by

$$\mathcal{M}_{\mathbf{k},\mathbf{r}}(\mathfrak{c}, \mathfrak{d}) = \left\{1 \leq e \leq \mathfrak{d} \colon\ \mathbf{k}(\mathfrak{c}, e; |\mathbf{r}| - 1) = \mathbf{k}\right\}.$$

For example, suppose $Q = 25$, $\mathfrak{c} = 1$, $\mathfrak{d} = 5$. One can find in $\mathfrak{F}^{25}$ the following series of consecutive fractions:

$$\ldots, \frac{7}{16}, \frac{11}{25}, \frac{4}{9}, \frac{9}{20}, \frac{5}{11}, \frac{11}{24}, \frac{6}{13}, \frac{7}{15}, \frac{8}{17}, \frac{9}{19}, \frac{10}{21}, \ldots$$

From these only $7/16, 5/11, 10/21$ survive, and are consecutive, in $\mathfrak{F}^{25}(1, 5)$. Then, in our terminology, the tuple of denominators $(16, 11, 21)$ is of type $\mathtt{T}(\mathbf{r})$, with $\mathbf{r} = (4, 6)$. In particular, we see that $r_1 - 1, \ldots, r_s - 1$ are, respectively, the number of denominators of consecutive fractions in $\mathfrak{F}^Q$ that are $\not\equiv \mathfrak{c} \pmod{\mathfrak{d}}$ intercalated between the fractions with denominators that are $\equiv \mathfrak{c} \pmod{\mathfrak{d}}$. Also, $\mathbf{k}(16, 25; 9) = (1, 5, 1, 4, 1, 3, 2, 2, 2, 2) \in \mathcal{A}_{\mathbf{r}}(1, 5)$ has $|\mathbf{r}| - 1 = 4 + 6 - 1 = 9$ components, and

$$F^Q_{\mathbf{r}}(16, 25) = \left(16, 11, 21\right).$$

3 Lattice Points in Plane Domains

Given a set $\Omega \subset \mathbb{R}^2$ and integers $0 \leq a, b < \mathfrak{d}$, let $N'_{a,b;\mathfrak{d}}(\Omega)$ be the number of lattice points in Ω with relatively prime coordinates congruent modulo $\mathfrak{d}$ to a, b, respectively, that is,

$$N'_{a,b;\mathfrak{d}}(\Omega) := \#\left\{(m, n) \in \Omega \colon\ m \equiv a \pmod{\mathfrak{d}};\ n \equiv b \pmod{\mathfrak{d}};\ \gcd(m, n) = 1\right\}.$$

[3] We write $\mathbf{q} \equiv \mathfrak{c} \pmod{\mathfrak{d}}$ if all the components of $\mathbf{q}$ are $\equiv \mathfrak{c} \pmod{\mathfrak{d}}$.

Notice that when $\gcd(a,b,\mathfrak{d}) > 1$, the set in the definition above is empty, so $N'_{a,b;\mathfrak{d}}(\Omega) = 0$.

Lemma 1. *Let $R > 0$ and let $\Omega \subset \mathbb{R}^2$ be a convex set of diameter $\le R$. Let $\mathfrak{d}$ be a positive integer and let $0 \le a, b < \mathfrak{d}$, with $\gcd(a,b,\mathfrak{d}) = 1$. Then*

$$N'_{a,b;\mathfrak{d}}(\Omega) = \frac{6}{\pi^2 \mathfrak{d}^2} \prod_{p|\mathfrak{d}} \left(1 - \frac{1}{p^2}\right)^{-1} \operatorname{Area}(\Omega) + O\big(R \log R\big) . \tag{2}$$

The proof follows by a standard argument, as in the proof of [2, Lemma 3.1].

As a consequence of Lemma 1, we obtain an asymptotic formula for the cardinality of $\mathfrak{F}^Q(\mathfrak{c},\mathfrak{d})$. For this we use (2) and two more facts. Firstly, the area of the Farey triangle is $\operatorname{Area}(\mathcal{T}^Q) = Q^2/2$ and secondly, $\#\mathfrak{F}^Q(\mathfrak{c},\mathfrak{d})$ is the number of lattice points $(a,b) \in \mathcal{T}^Q \times \mathcal{T}^Q$ with relatively prime coordinates, $a \equiv \mathfrak{c} \pmod{d}$, and no other condition on b. Since the number of integers $0 \le e < \mathfrak{d}$ for which $\gcd(\mathfrak{c}, e, \mathfrak{d}) = 1$ is $\mathfrak{d} \cdot \varphi(\gcd(\mathfrak{c},\mathfrak{d}))/\gcd(\mathfrak{c},\mathfrak{d})$, it follows that

$$\#\mathfrak{F}^Q(\mathfrak{c},\mathfrak{d}) = \frac{3Q^2}{\pi^2} \cdot \frac{\varphi(\gcd(\mathfrak{c},\mathfrak{d}))}{\gcd(\mathfrak{c},\mathfrak{d})\mathfrak{d}} \prod_{p|\mathfrak{d}} \left(1 - \frac{1}{p^2}\right)^{-1} + O\big(\mathfrak{d} Q \log Q\big) . \tag{3}$$

4 The Density of Points of type $\mathtt{T}(\mathbf{r})$

We count separately the contribution to $g_s(\mathbf{x};\mathfrak{c},\mathfrak{d})$ of points of the same type. Thus, we denote by $g_{\mathbf{r}}(\mathbf{x}) = g_{\mathbf{r}}(\mathbf{x};\mathfrak{c},\mathfrak{d})$, the local density in the unit cube $[0,1]^{s+1}$ of the points $(q_0/Q, q_1/Q, \ldots, q_s/Q)$ of type $\mathtt{T}(\mathbf{r})$, as $Q \to \infty$. At any point $\mathbf{u} = (u_0, \ldots, u_s) \in [0,1]^{s+1}$, this local density $g_{\mathbf{r}}(\mathbf{u})$ is defined by

$$g_{\mathbf{r}}(\mathbf{u}) := \lim_{\eta \to 0} \frac{\lim\limits_{Q\to\infty} \frac{\#\left(\square \cap \mathcal{D}^Q_{\mathbf{r}}(\mathfrak{c},\mathfrak{d})/Q\right)}{\#\mathcal{D}^Q_s(\mathfrak{c},\mathfrak{d})}}{4\eta^2} , \tag{4}$$

where

$$\mathcal{D}^Q_{\mathbf{r}}(\mathfrak{c},\mathfrak{d}) := \left\{ (q^0, q^1, \ldots, q^s) \text{ of type } \mathtt{T}(\mathbf{r}) \colon \begin{array}{l} q^0, q^1, \ldots, q^s \text{ are denominators of} \\ \text{consecutive fractions in } \mathfrak{F}^Q(\mathfrak{c},\mathfrak{d}) \end{array} \right\},$$

and $\square \subset \mathbb{R}^{s+1}$ are cubes of edge 2η centered at $\mathbf{u}$. Then, we have

$$g_s(\mathbf{u}) = \sum_{\mathbf{r}} g_{\mathbf{r}}(\mathbf{u}) , \tag{5}$$

provided we show that each local density $g_{\mathbf{r}}(\mathbf{u})$ exists, as $Q \to \infty$. In the following we find each $g_{\mathbf{r}}(\mathbf{u})$.

5 The Witness Set

Let $\eta > 0$ be small and let $\mathbf{x}^0 = (x^0_0, \ldots, x^0_s) \in [0,1]^{s+1}$ be the point around which we check the density. We consider the parallelepiped centered at $\mathbf{x}^0$ and edge 2η given by

$\square = \square_\eta(\mathbf{x}^0) = (x_0^0 - \eta, x_0^0 + \eta) \times \cdots \times (x_s^0 - \eta, x_s^0 + \eta)$. Then, given $\mathbf{r} = (r_1, \ldots, r_s)$, we need to estimate the cardinality of

$$\mathcal{B}_{\mathbf{r}}^Q(\mathfrak{c}, \mathfrak{d}) = \left\{ (q', q'') \in \mathbb{N}^2 \colon \begin{array}{c} 1 \le q', q'' \le Q,\ \gcd(q', q'') = 1,\ q' + q'' > Q, \\ \mathbf{k}(q', q''; |\mathbf{r}| - 1) \in \mathcal{A}_{\mathbf{r}}(\mathfrak{c}, \mathfrak{d}),\ F_{\mathbf{r}}^Q(q', q'') \in Q \cdot \square \end{array} \right\}.$$

This reduces to an area estimate if we put

$$\Omega_{\mathbf{r}}^Q(\mathfrak{c}, \mathfrak{d}) = \left\{ (x, y) \in [1, Q]^2 \colon \begin{array}{l} x + y > Q, \\ \mathbf{k}(x, y; |\mathbf{r}| - 1) \in \mathcal{A}_{\mathbf{r}}(\mathfrak{c}, \mathfrak{d}),\ F_{\mathbf{r}}^Q(x, y) \in Q \cdot \square \end{array} \right\}.$$

Then, by Lemma 1,

$$\begin{aligned} \#\mathcal{B}_{\mathbf{r}}^Q(\mathfrak{c}, \mathfrak{d}) &= \sum_{e \in \mathcal{M}_{\mathbf{k},\mathbf{r}}(\mathfrak{c},\mathfrak{d})} N'_{\mathfrak{c},e;\mathfrak{d}}\big(\Omega_{\mathbf{r}}^Q(\mathfrak{c}, \mathfrak{d})\big) \\ &= \frac{6}{\pi^2 \mathfrak{d}^2} Q^2 \prod_{p \mid \mathfrak{d}} \left(1 - \frac{1}{p^2}\right)^{-1} \sum_{e \in \mathcal{M}_{\mathbf{k},\mathbf{r}}(\mathfrak{c},\mathfrak{d})} \operatorname{Area}\big(\Omega_{\mathbf{r}}(\mathfrak{c}, \mathfrak{d})\big) + O\big(\mathfrak{d} Q \log Q\big), \end{aligned} \tag{6}$$

where

$$\Omega_{\mathbf{r}}(\mathfrak{c}, \mathfrak{d}) = \left\{ (x, y) \in (0, 1]^2 \colon \begin{array}{l} x + y > 1, \\ \mathbf{k}(x, y; |\mathbf{r}| - 1) \in \mathcal{A}_r(\mathfrak{c}, \mathfrak{d}),\ F_{\mathbf{r}}(x, y) \in \square \end{array} \right\}.$$

For any $\mathbf{k}$, we denote

$$\mathcal{T}_{\mathbf{k}} := \big\{ (x, y) \in (0, 1]^2 \colon\ x + y > 1,\ \mathbf{k}(x, y; |\mathbf{r}| - 1) = \mathbf{k} \big\}$$

and

$$\mathcal{P}_{\mathbf{k}}(\eta) := \big\{ (x, y) \in (0, 1]^2 \colon\ F_{\mathbf{r}}(x, y) \in \square \big\}. \tag{7}$$

Notice that the dependence on $\mathbf{k}$ of the set $\mathcal{P}_{\mathbf{k}}(\eta)$ is through the components of $F_{\mathbf{r}}(x, y)$ (see (11) below). Also, we put $\mathcal{T}_0 := \mathcal{T}$, the Farey triangle.

Then, we have

$$\operatorname{Area}\big(\Omega_{\mathbf{r}}(\mathfrak{c}, \mathfrak{d})\big) = \sum_{\mathbf{k} \in \mathcal{A}_{\mathbf{r}}(\mathfrak{c},\mathfrak{d})} \operatorname{Area}\big(\mathcal{T}_{\mathbf{k}} \cap \mathcal{P}_{\mathbf{k}}(\eta)\big). \tag{8}$$

By a compactness argument it follows that only finitely many terms of the series are non-zero, although $\mathcal{A}_{\mathbf{r}}(\mathfrak{c}, \mathfrak{d})$ may be infinite. Next we need to see the shape of $\mathcal{P}_{\mathbf{k}}(\eta)$, since we are mainly interested to know $\operatorname{Area}\big(\mathcal{P}_{\mathbf{k}}(\eta)\big)$. This is the object of the next section.

6 The index $p_r(\mathbf{k})$ and the polygon $\mathcal{P}_{\mathbf{k}}(\eta)$

The integer values k_j defined in Section 2 satisfy the classical *mediant* property of the Farey series. For instance, if q', q'', q''' are consecutive denominators of three fractions in $\mathfrak{F}^Q$, then $k := (q' + q''')/q''$ is a positive integer. Hall and Shiu [15] called it the *index* of the fractions with denominators q', q'', respectively.

More generally, for a series of indexes $k_1, k_2, \dots$, we consider a sequence of polynomials $p_j(\cdot)$, defined as follows. Let $p_{-1}(\cdot) = 0$, $p_0(\cdot) = 1$, and then, for any $j \geq 1$,

$$p_j(k_1, \dots, k_j) = k_j p_{j-1}(k_1, \dots, k_{j-1}) - p_{j-2}(k_1, \dots, k_{j-2}). \tag{9}$$

The first polynomials with nonempty argument are:

$$\begin{aligned}
p_1(\mathbf{k}) &= k_1;\\
p_2(\mathbf{k}) &= k_1 k_2 - 1;\\
p_3(\mathbf{k}) &= k_1 k_2 k_3 - k_1 - k_3;\\
p_4(\mathbf{k}) &= k_1 k_2 k_3 k_4 - k_1 k_2 - k_1 k_4 - k_3 k_4 + 1;\\
p_5(\mathbf{k}) &= k_1 k_2 k_3 k_4 k_5 - k_1 k_2 k_3 - k_1 k_2 k_5 - k_1 k_4 k_5 - k_3 k_4 k_5 + k_1 + k_3 + k_5.
\end{aligned}$$

Often we write $\mathbf{k}$, meaning the whole sequence of indexes starting with k_1, but notice that the polynomial of rank j depends only on the first variables $k_1, \dots, k_j$. In particular, one sees that $p_1(\mathbf{k}) = k_1$ coincides with the index of Hall and Shiu. Also, we remark the symmetry property:

$$p_j(k_j, \dots, k_1) = p_j(k_1, \dots, k_j), \quad \text{for } j \geq 1\,. \tag{10}$$

The role played by these polynomials is revealed by the next relation, which shows that for any $j \geq -1$, $x_j^{\mathcal{L}}(x, y)$ is a linear combination of x and y:

$$x_j^{\mathcal{L}}(x, y) = p_j(k_1, \dots, k_j) y - p_{j-1}(k_2, \dots, k_j) x\,. \tag{11}$$

Turning now to the set $\mathcal{P}_{\mathbf{k}}(\eta)$ defined by (7), where $\mathbf{k} = \mathbf{k}(x, y; |\mathbf{r}| - 1)$, by (11) we see that this is the set of points $(x, y) \in \mathbb{R}^2$ that satisfy simultaneously the conditions:

$$\begin{cases}
x_0^0 - \eta < x < x_0^0 + \eta,\\
x_1^0 - \eta < p_{r_1-1}(k_1, \dots, k_{r_1-1}) y - p_{r_1-2}(k_2, \dots, k_{r_1-1}) x < x_1^0 + \eta,\\
x_2^0 - \eta < p_{r_1+r_2-1}(k_1, \dots, k_{r_1+r_2-1}) y - p_{r_1+r_2-2}(k_2, \dots, k_{r_1+r_2-1}) x < x_2^0 + \eta,\\
\qquad\vdots\\
x_s^0 - \eta < p_{|\mathbf{r}|-1}(k_1, \dots, k_{|\mathbf{r}|-1}) y - p_{|\mathbf{r}|-2}(k_2, \dots, k_{|\mathbf{r}|-1}) x < x_s^0 + \eta\,.
\end{cases} \tag{12}$$

This shows that $\mathcal{P}_{\mathbf{k}}(\eta)$ is the intersection of $s+1$ strips and for $\eta_1, \eta_2 > 0$ the sets $\mathcal{P}_{\mathbf{k}}(\eta_1)$ and $\mathcal{P}_{\mathbf{k}}(\eta_2)$ are similar, the ratio of similarity being equal to η_1/η_2. Consequently, it follows that

$$\operatorname{Area}(\mathcal{P}_{\mathbf{k}}(\eta)) = \eta^2 \operatorname{Area}(\mathcal{P}_{\mathbf{k}}(1))\,, \tag{13}$$

and $\operatorname{Area}\big(\mathcal{P}_{\mathbf{k}}(1)\big)$ is independent of η.

In particular, in the case $s = 1$, for $\mathbf{k} = (k_1, \dots, k_{r_1-1})$, the set $\mathcal{P}_{\mathbf{k}}(\eta)$ is a parallelogram of center

$$C_{\mathbf{k}} = \left(x_0^0,\ \frac{p_{r_1-2}(k_2, \dots, k_{r_1-1})}{p_{r_1-1}(k_1, \dots, k_{r_1-1})} x_0^0 + \frac{1}{p_{r_1-1}(k_1, \dots, k_{r_1-1})} x_1^0 \right), \tag{14}$$

and area

$$\operatorname{Area}(\mathcal{P}_{\mathbf{k}}(\eta)) = \frac{4\eta^2}{p_{r_1-1}(\mathbf{k})}\,. \tag{15}$$

7 The Density of Points of Type $\mathtt{T}(\mathbf{r})$

The variable $\eta > 0$ is for now fixed, but eventually will tend to zero. When $\eta \downarrow 0$, for each $\mathbf{k}$ the polygons $\mathcal{P}_{\mathbf{k}}(\eta)$ are smaller and smaller and converge toward a point $C_{\mathbf{k}}$, which we call the *core* of $\mathcal{P}_{\mathbf{k}}(\eta)$. If $s = 1$, $\mathcal{P}_{\mathbf{k}}(\eta)$ is a parallelogram and the core of $\mathcal{P}_{\mathbf{k}}(\eta)$ coincides with its center given by (14).

Suppose now that $\mathbf{k} \in \mathcal{A}_{\mathbf{r}}(\mathfrak{c}, \mathfrak{d})$ is fixed. The size of $\operatorname{Area}\big(\mathcal{T}_{\mathbf{k}} \cap \mathcal{P}_{\mathbf{k}}(\eta)\big)$ depends on the position of the core with respect to $\mathcal{T}_{\mathbf{k}}$. There are three cases.

If $C_{\mathbf{k}} \in \mathring{\mathcal{T}}_{\mathbf{k}}$,[4] then, for η small enough, $\mathcal{P}_{\mathbf{k}}(\eta) \subset \mathcal{T}_{\mathbf{k}}$, so $\operatorname{Area}\big(\mathcal{T}_{\mathbf{k}} \cap \mathcal{P}_{\mathbf{k}}(\eta)\big) = \operatorname{Area}(\mathcal{P}_{\mathbf{k}}(\eta))$. Then, by (13), we get

$$\operatorname{Area}(\mathcal{T}_{\mathbf{k}} \cap \mathcal{P}_{\mathbf{k}}(\eta)) = \eta^2 \operatorname{Area}(\mathcal{P}_{\mathbf{k}}(1))\,, \quad \text{if } C_{\mathbf{k}} \in \mathring{\mathcal{T}}_{\mathbf{k}}. \tag{16}$$

Suppose now that $C_{\mathbf{k}} \in \partial\mathcal{T}_{\mathbf{k}} \setminus V(\mathcal{T}_{\mathbf{k}})$. Then there exists a certain bound η_1 such that if $\eta < \eta_1$, the intersections $\mathcal{B}_{\mathbf{k}}(\eta) = \mathcal{T}_{\mathbf{k}} \cap \mathcal{P}_{\mathbf{k}}(\eta)$ are polygons similar to each other. Let $B_{\mathbf{k}}$ be the polygon similar to these ones for which the variable η equals 1 in all the equations of the boundaries of the strips from (12), whose intersection is $\mathcal{P}_{\mathbf{k}}(\eta)$. So, the size of $B_{\mathbf{k}}$ is independent of η. Notice that $\mathcal{B}_{\mathbf{k}}$ is generally smaller than $\mathcal{P}_{\mathbf{k}}(1)$, and even smaller than $\mathcal{T}_{\mathbf{k}} \cap \mathcal{P}_{\mathbf{k}}(1)$. Then, we have

$$\operatorname{Area}(\mathcal{T}_{\mathbf{k}} \cap \mathcal{P}_{\mathbf{k}}(\eta)) = \eta^2 \operatorname{Area}(\mathcal{B}_{\mathbf{k}})\,, \quad \text{if } C_{\mathbf{k}} \in \partial\mathcal{T}_{\mathbf{k}} \setminus V(\mathcal{T}_{\mathbf{k}}) \text{ and } \eta < \eta_1. \tag{17}$$

If $C_{\mathbf{k}} \in V(\mathcal{T}_{\mathbf{k}})$, the reasoning from the previous case shows that there exists $\eta_2 > 0$, with the property that for $\eta_2 < \eta$ the polygons $\mathcal{V}_{\mathbf{k}}(\eta) = \mathcal{T}_{\mathbf{k}} \cap \mathcal{P}_{\mathbf{k}}(\eta)$ are similar to each other. Then, we denote by $\mathcal{V}_{\mathbf{k}}$ the polygon similar to these ones for which $\eta = 1$ in all the equations of the boundaries of the strips from (12). Let us observe that the size of $\mathcal{V}_{\mathbf{k}}$ is independent of η, and although we use the same notation, the polygons $\mathcal{V}_{\mathbf{k}}$ are distinct for different vertices of $\mathcal{T}_{\mathbf{k}}$. These yield

$$\operatorname{Area}(\mathcal{T}_{\mathbf{k}} \cap \mathcal{P}_{\mathbf{k}}(\eta)) = \eta^2 \operatorname{Area}(\mathcal{V}_{\mathbf{k}})\,, \quad \text{if } C_{\mathbf{k}} \in V(\mathcal{T}_{\mathbf{k}}) \text{ and } \eta < \eta_2. \tag{18}$$

Inserting the evaluations from (16), (17) and (18) into (8), for $0 < \eta < \max(\eta_1, \eta_2)$ it yields

$$\begin{aligned}\operatorname{Area}\big(\Omega_{\mathbf{r}}(\mathfrak{c}, \mathfrak{d})\big) =& \eta^2 \sum_{C_{\mathbf{k}} \in \mathring{\mathcal{T}}_{\mathbf{k}}} \operatorname{Area}\big(\mathcal{P}_{\mathbf{k}}(1)\big) + \eta^2 \sum_{C_{\mathbf{k}} \in \partial\mathcal{T}_{\mathbf{k}} \setminus V(\mathcal{T}_{\mathbf{k}})} \operatorname{Area}(\mathcal{B}_{\mathbf{k}}) \\ &+ \eta^2 \sum_{C_{\mathbf{k}} \in V(\mathcal{T}_{\mathbf{k}})} \operatorname{Area}(\mathcal{V}_{\mathbf{k}})\,.\end{aligned} \tag{19}$$

Since the number of tuples $(q_0, \ldots, q_s)$ of consecutive denominators of fractions in $\mathfrak{F}^Q(\mathfrak{c}, \mathfrak{d})$

[4] For a polygon $\mathcal{P} \subset \mathbb{R}^2$, we denote by $\mathring{\mathcal{P}}$, $\partial\mathcal{P}$ and $V(\mathcal{P})$, the topological interior, the boundary, and the set of vertices of $\mathcal{P}$, respectively.

is $\#\mathfrak{F}^Q(\mathfrak{c},\mathfrak{d}) + O(1)$, making use of (6) and (3), it follows that

$$\begin{aligned}\int\limits_{\square_\eta(\mathbf{x}^0)} g_{\mathbf{r}}(\mathbf{x})\, d\mathbf{x} &= \iint\limits_{\square_\eta(\mathbf{x}^0)\cap F_{\mathbf{r}}(\mathcal{T})} g_{\mathbf{r}}\big(\mathbf{x}^{\mathcal{L}}(x,y)\big)\, dxdy = \lim_{Q\to\infty} \frac{\#\mathcal{B}_{\mathbf{r}}^Q(\mathfrak{c},\mathfrak{d})}{\#\mathfrak{F}^Q(\mathfrak{c},\mathfrak{d})} \\ &= \frac{2\gcd(\mathfrak{c},\mathfrak{d})}{\mathfrak{d}\varphi(\gcd(\mathfrak{c},\mathfrak{d}))} \sum_{e\in\mathcal{M}_{\mathbf{k},\mathbf{r}}(\mathfrak{c},\mathfrak{d})} \operatorname{Area}\big(\Omega_{\mathbf{r}}(\mathfrak{c},\mathfrak{d})\big)\,.\end{aligned} \tag{20}$$

By Lebesgue differentiation, combining (20) and (19), we get the following result.

Theorem 1. *Let $\mathfrak{d}\ge 2$ and $0\le\mathfrak{c}\le\mathfrak{d}-1$ be integers. Then, for any $\mathbf{x}^0 = (x_0^0, x_1^0,\dots,x_s^0)\in[0,1]^{s+1}$, we have:*

$$\begin{aligned} g_{\mathbf{r}}(\mathbf{x}^0) = \frac{\gcd(\mathfrak{c},\mathfrak{d})}{2\mathfrak{d}\varphi(\gcd(\mathfrak{c},\mathfrak{d}))}\Bigg(&\sum_{e\in\mathcal{M}_{\mathbf{k},\mathbf{r}}(\mathfrak{c},\mathfrak{d})} \sum_{C_{\mathbf{k}}\in\mathring{\mathcal{T}}_{\mathbf{k}}} \operatorname{Area}\big(\mathcal{P}_{\mathbf{k}}(1)\big) + \sum_{C_{\mathbf{k}}\in\partial\mathcal{T}_{\mathbf{k}}\setminus V(\mathcal{T}_{\mathbf{k}})} \operatorname{Area}(\mathcal{B}_{\mathbf{k}}) \\ &+ \sum_{C_{\mathbf{k}}\in V(\mathcal{T}_{\mathbf{k}})} \operatorname{Area}(\mathcal{V}_{\mathbf{k}})\Bigg),\end{aligned} \tag{21}$$

where the sums run over tuples $\mathbf{k}\in\mathcal{A}_{\mathbf{r}}(\mathfrak{c},\mathfrak{d})$.

We remark that in (21), the first term is essential, since it gives the local density on $[0,1]^{s+1}$, except on a set of area zero.

8 The existence of $g_s(\mathbf{x})$ and of $\mathcal{D}_s(\mathfrak{c},\mathfrak{d})$

Putting together the contribution of points of all types, by (4) and Theorem 1, we get the main result below.

Theorem 2. *Let $\mathfrak{d}\ge 2$ and $0\le\mathfrak{c}\le\mathfrak{d}-1$ be integers. Then, for any $\mathbf{x}=(x_0,x_1,\dots,x_s)\in[0,1]^{s+1}$, we have*

$$\begin{aligned} g_s(\mathbf{x}) = &\frac{\gcd(\mathfrak{c},\mathfrak{d})}{2\mathfrak{d}\varphi(\gcd(\mathfrak{c},\mathfrak{d}))} \sum_{\mathbf{r}} \sum_{\mathbf{k}\in\mathcal{A}_{\mathbf{r}}(\mathfrak{c},\mathfrak{d})} \sum_{e\in\mathcal{M}_{\mathbf{k},\mathbf{r}}(\mathfrak{c},\mathfrak{d})} \sum_{C_{\mathbf{k}}\in\mathring{\mathcal{T}}_{\mathbf{k}}} \operatorname{Area}\big(\mathcal{P}_{\mathbf{k}}(1)\big) \\ &+ \frac{\gcd(\mathfrak{c},\mathfrak{d})}{2\mathfrak{d}\varphi(\gcd(\mathfrak{c},\mathfrak{d}))} \sum_{\mathbf{r}} \sum_{\mathbf{k}\in\mathcal{A}_{\mathbf{r}}(\mathfrak{c},\mathfrak{d})} \sum_{C_{\mathbf{k}}\in\partial\mathcal{T}_{\mathbf{k}}\setminus V(\mathcal{T}_{\mathbf{k}})} \operatorname{Area}(\mathcal{B}_{\mathbf{k}}) \\ &+ \frac{\gcd(\mathfrak{c},\mathfrak{d})}{2\mathfrak{d}\varphi(\gcd(\mathfrak{c},\mathfrak{d}))} \sum_{\mathbf{r}} \sum_{\mathbf{k}\in\mathcal{A}_{\mathbf{r}}(\mathfrak{c},\mathfrak{d})} \sum_{C_{\mathbf{k}}\in V(\mathcal{T}_{\mathbf{k}})} \operatorname{Area}(\mathcal{V}_{\mathbf{k}}).\end{aligned}$$

As a consequence, we obtain as a natural object the support set.

Corollary 1. *There exists a limiting set $\mathcal{D}_s(\mathfrak{c},\mathfrak{d}) := \lim_{Q\to\infty}\mathcal{D}_s(\mathfrak{c},\mathfrak{d})/Q$, as $Q\to\infty$.*

When $s=1$, the theorem can be stated more precisely using (15).

Corollary 2. *Let $\mathfrak{d} \geq 2$ and $0 \leq \mathfrak{c} \leq \mathfrak{d} - 1$ be integers. Then, for any $(x, y) \in [0, 1]^2$, we have*

$$\begin{aligned} g_1(x,y) =& \frac{2\gcd(\mathfrak{c},\mathfrak{d})}{\mathfrak{d}\varphi(\gcd(\mathfrak{c},\mathfrak{d}))} \sum_{e\in\mathcal{M}_{\mathbf{k},r}(\mathfrak{c},\mathfrak{d})} \sum_{C_{\mathbf{k}}\in\overset{\circ}{\mathcal{T}_{\mathbf{k}}}} \frac{1}{p_{r-1}(\mathbf{k})} + \frac{\gcd(\mathfrak{c},\mathfrak{d})}{\mathfrak{d}\varphi(\gcd(\mathfrak{c},\mathfrak{d}))} \sum_{C_{\mathbf{k}}\in\partial\mathcal{T}_{\mathbf{k}}\setminus V(\mathcal{T}_{\mathbf{k}})} \frac{1}{p_{r-1}(\mathbf{k})} \\ &+ \frac{\gcd(\mathfrak{c},\mathfrak{d})}{2\mathfrak{d}\varphi(\gcd(\mathfrak{c},\mathfrak{d}))} \sum_{C_{\mathbf{k}}\in V(\mathcal{T}_{\mathbf{k}})} \mathrm{Area}(\mathcal{V}_{\mathbf{k}}), \end{aligned} \tag{22}$$

where the sums run over all $r \geq 1$ and $\mathbf{k} \in \mathcal{A}_r(\mathfrak{c}, \mathfrak{d})$.

Corollary 2 with $\mathfrak{d} = 2$ retrieves the authors' previous result [11, Theorem 3] as a particular instance.

9 The Mosaics

The noteworthy thing hidden in the background of Theorem 2 is the geometry of the arrangements of the domains $F_{\mathbf{r}}(\mathcal{T}_{\mathbf{k}})$, which we call *pieces* or *tiles*. It is easier to see this in the bidimensional case, $s = 1$, assumed in what follows. Then the tiles are polygons included in $[0, 1]^2$ and the choice application becomes

$$F_n(x,y) = \left(x, x_n^{\mathcal{L}}(x,y)\right), \quad \text{for } n \geq 1\,.$$

For any $\mathbf{k} = (k_1, \ldots, k_n)$, we shall call *kernel* the integer $p_n(\mathbf{k})$. Moreover, we say that it is the kernel of the tile $F_n(\mathcal{T}_{\mathbf{k}})$. Notice that the inverse of the kernel is the contribution of each $\mathbf{k}$ to $g_1(x, y)$. The tiles of a given kernel fit into a few larger polygons, which we call *mosaics*. Their common feature is that always one of their vertices is at $(1, 1)$. They are either symmetric with respect to the first diagonal or they appear in pairs, symmetric to each other with respect to the first diagonal. Most of them are quadrangles, but their shape may vary a lot with $\mathfrak{d}$, $\mathfrak{c}$ and the value of the kernel.

These mosaics behave like successive layers of constant density put over $[0, 1]^2$. Then the local density $g_1(x, y)$ at a given point $(x, y) \in [0, 1]^2$ is the sum of the densities on the mosaics (the inverse of its kernel) stung by (x, y). The contribution to the sum is halved if (x, y) touches only an edge of a mosaic, and if the point touches a vertex of a mosaic, it adds to the sum the density reduced proportionally with the size of the angle of the mosaic at that vertex. The number of mosaics that lay over $(x, y) \neq (1, 1)$ is finite, and it is endless if $(x, y) = (1, 1)$.

For each given $\mathfrak{c}, \mathfrak{d}$, the number of the mosaics is unbounded, but their size has a certain rate of decay as their kernel increases. In the Appendix we have included the larger mosaics in two moduli: $\mathfrak{d} = 5$ and $\mathfrak{d} = 12$.

It seems that the set $\mathcal{D}_1(\mathfrak{c}, \mathfrak{d})$ is always equal to the first mosaic, which happens to be the largest. This is known to be true when $\mathfrak{d}$ is small and in the cases $\mathfrak{c} = 0$ and $\mathfrak{d}$ prime [12]. Many other intriguing questions are raised by these objects. Here, we conclude only by pointing out that each of these mosaics has an associated tree. In the nodes the tree has the tuples $\mathbf{k}$ that define the tiles and the arcs link nodes whose corresponding tiles are adjacent on the mosaic. The root node corresponds to the tile with a vertex at $(1, 1)$. As an example, in Figure 1, it is the tree associated with the mosaic $SQ_1[9]$ from Figure 11.

10 Acknowledgments

The authors are grateful to the referees for their very useful comments and suggestions.

11 Appendix–The Plane-mosaics in the cases $\mathfrak{c} = 1, 2, 3, 4;\ \mathfrak{d} = 5$ and $\mathfrak{c} = 3;\ \mathfrak{d} = 12$

We have assigned names to the mosaics using the following conventions. The first letter is either S or N, according to whether the mosaic is or is not symmetric with respect to the first diagonal. Since the non-symmetric ones appear in pairs, symmetric to each other with respect to the first diagonal, we have included the picture of only one of them. The next letter or group of letters indicates the shape of the mosaic. The possible configuration are: triangle (T), quadrangle (Q), pentagon (P), hexagon (H), octagon (O) or concave hexagon–V-shape (V). The argument is the tuple $\mathbf{k}$ that gives the tile from the North-East corner. Finally, the subscript represents the number of components of $\mathbf{k}$.

For example, the mosaic $NP_3[2,2,3]$ (see Figure 8) is a non-symmetric pentagon, whose tile from the N-E corner is the transformation of $\mathcal{T}_{2,2,3}$ through $F_3(x,y)$, and $SQ_1[6]$ (Figure 15) is a symmetric quadrangle, whose piece from the N-E corner is the image of $\mathcal{T}_6$ through $F_1(x,y)$.

As an exemplification, in Figure 1 we have included merely a tree associated with a mosaic. There, nodes are the tuples $\mathbf{k}$ defining the tiles of $NP_3[2,2,3]$ and the arcs connect tuples $\mathbf{k}$ that define adjacent tiles of the mosaic from Figure 8.

More data on the mosaics are entered in Tables 1 and 2. On the first column, one can find the kernel, the number whose inverse gives the local density on the layer given by that mosaic. The entry on the third column is the number of tiles arranged in the mosaic, while on the forth are the orders–the number of components–of $\mathbf{k}$'s (the smallest and the largest) that produce the tiles. In the last column are the coordinates of the vertices of the mosaic.

In the pictures we have used the same color to indicate the chains of tiles with $\mathbf{k}$'s of the same orders. There, always neighbor chains have orders of $\mathbf{k}$'s that differ by exactly one.

For the modulus $\mathfrak{d} = 5$, the mosaics are the same in any of the cases $\mathfrak{c} = 1, 2, 3$ or 4, but they are different when $\mathfrak{c} = 0$. When $\mathfrak{d} = 12$, the situation is more complex, mainly due to the larger number of factors of 12. Due to arithmetical constraints, there are no mosaics of kernel 2 when $\mathfrak{d} = 5$ and $\mathfrak{c} = 1, 2, 3$ or 4.

We remark that $\mathcal{D}_1(\mathfrak{c}, 5) = SQ_0[\cdot]$, for $\mathfrak{c} = 1, 2, 3$ or 4 and $\mathcal{D}_1(3, 12) = SH_1[3]$. In other words, this says that the limiting set of pairs of consecutive denominators from $\mathfrak{F}^Q(\mathfrak{c}, \mathfrak{d})$ equals, as $Q \to \infty$, the largest of the mosaics.

Finally, we mention that $\mathcal{D}_1(3, 12)$ is the first case in which $\mathcal{D}_1(\mathfrak{c}, \mathfrak{d})$ is an hexagon, as for any $\mathfrak{d} \leq 11$ and $0 \leq \mathfrak{c} \leq \mathfrak{d}$ the set $\mathcal{D}_1(\mathfrak{c}, \mathfrak{d})$ has a quadrangular form.

Table 1: The mosaics in the cases $\mathfrak{d} = 5$, $\mathfrak{c} = 1, 2, 3$ or 4.

Kernel	Name	No. of tiles	Orders	Vertices of the mosaic
1	$SQ_0[\cdot]$	21	$0-9$	$(1,1); (0,1); (1/6,1/6); (1,0)$
2	$-$	$-$	$-$	$-$
3	$SQ_1[3]$	7	$1-5$	$(1,1); (2/7,1); (3/8,3/8); (1,2/7)$
4	$SQ_1[4]$	27	$1-11$	$(1,1); (3/13,1); (2/7,2/7); (1,3/13)$
5	$SHV_4[2,2,2,2]$	35	$4-14$	$(1,1); (1/6,1); (8/43,23/43); (1/2,1/2); (23/43,8/43); (1,1/6)$
6	$SH_1[6]$	51	$1-11$	$(1,1); (1/5,1); (4/19,14/19); (3/8,3/8); (14/19,4/19); (1,1/5)$
7	$NQ_2[2,4]$	6	$2-6$	$(1,1); (6/11,1); (3/5,2/5); (1,3/8)$
7	$NQ_2[4,2]$	6	$2-6$	$(1,1); (3/8,1); (2/5,3/5); (1,6/11)$
7	$NP_3[2,2,3]$	30	$3-12$	$(1,1); (3/13,1); (7/17,7/17); (4/5,1/5); (1,6/31)$
7	$NP_3[3,2,2]$	30	$3-12$	$(1,1); (6/31,1); (1/5,4/5); (7/17,7/17); (1,3/13)$
8	$SQ_1[8]$	21	$1-9$	$(1,1); (7/17,1); (4/9,4/9); (1,7/17)$
8	$SH_3[2,3,2]$	36	$3-13$	$(1,1); (7/37,1); (6/31,26/31); (4/9,4/9); (26/31,6/31); (1,7/37)$
9	$SQ_1[9]$	33	$1-9$	$(1,1); (2/7,1); (9/19,9/19); (1,2/7)$
9	$NP_4[2,2,2,3]$	7	$4-15$	$(1,1); (8/43,1); (7/37,32/37); (1/3,2/3); (1,5/7)$
9	$NP_4[3,2,2,2]$	7	$4-15$	$(1,1); (5/7,1); (2/3,1/3); (32/37,7/37); (1,8/43)$
...	...	...	...	...

Fig. 1: The tree of **k**'s associated with the mosaic $NP_3[2,2,3]$ ($\mathfrak{c} = 1, 2, 3$ or 4 and $\mathfrak{d} = 5$).

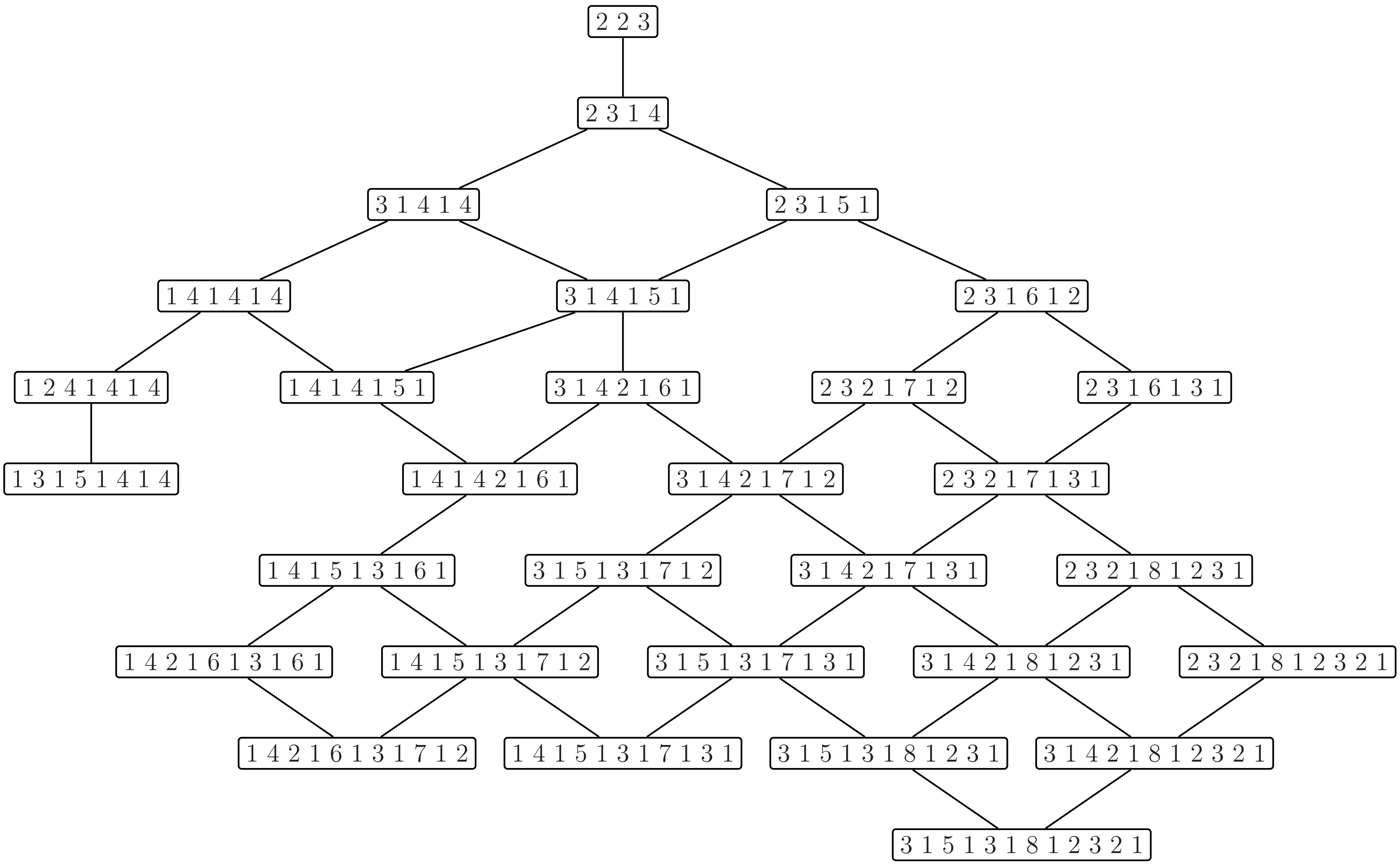

Table 2: The mosaics in the case $\mathfrak{d} = 12$, $\mathfrak{c} = 3$.

Kernel	Name	No. of tiles	Orders	Vertices of the mosaic
3	$SH_1[3]$	∞	$1 - \infty$	$(1,1); (0,1); (1/13,5/13); (1/5,1/5); (5/13,1/13); (1,0)$
3	$SQ_2[2,2]$	∞	$2 - \infty$	$(1,1); (0,1); (1/5,1/5); (1,0)$
6	$SQ_1[6]$	314	$1 - 41$	$(1,1); (1/9,1); (1/5,1/5); (1,1/9)$
6	$SH_5[2,2,2,2,2]$	424	$5 - 39$	$(1,1); (1/13,1); (1/9,5/9); (1/5,1/5); (5/9,1/9); (1,1/13)$
9	$SQ_1[9]$	63	$1 - 13$	$(1,1); (1/5,1); (3/7,3/7); (1,1/5)$
9	$NQ_4[2,2,2,3]$	56	$4 - 18$	$(1,1); (1/5,1); (1/4,1/2); (1,1/5)$
9	$NQ_4[3,2,2,2]$	56	$4 - 18$	$(1,1); (1/5,1); (1/2,1/4); (1,1/5)$
12	$SO_5[3,1,6,1,3]$	142	$5 - 29$	$(1,1); (1/5,1); (3/11,7/11); (4/13,8/13); (1/3,1/3); (8/13,4/13); (7/11,3/11); (1,1/5)$
12	$SQ_{11}[2,\ldots,2]$	21	$11 - 20$	$(1,1); (1/5,1); (1/2,1/2); (1,1/5)$
15	$SQ_1[15]$	38	$1 - 11$	$(1,1); (3/7,1); (5/9,5/9); (1,3/7)$
15	$SH_7[2,3,1,5,1,3,2]$	173	$7 - 29$	$(1,1); (1/4,1); (3/11,7/11); (5/13,5/13); (7/11,3/11); (1,1/4)$
15	$NQ_4[3,2,1,10]$	117	$4 - 27$	$(1,1); (3/11,1); (5/13,5/13); (1,1/3)$
15	$NQ_4[10,1,2,3]$	117	$4 - 27$	$(1,1); (1/3,1); (5/13,5/13); (1,3/11)$
15	$NQ_7[3,2,2,2,2,2,2]$	35	$7 - 20$	$(1,1); (1/3,1); (7/19,11/19); (1,1/2)$
15	$NQ_7[2,2,2,2,2,2,3]$	35	$7 - 20$	$(1,1); (1/2,1); (11/19,7/19); (1,1/3)$
18	$SQ_1[18]$	246	$1 - 26$	$(1,1); (1/5,1); (3/7,3/7); (1,1/5)$
18	$NQ_6[2,3,1,5,1,4]$	128	$6 - 28$	$(1,1); (1/5,1); (3/7,3/7); (1,5/13)$
18	$NQ_6[4,1,5,1,3,2]$	128	$6 - 28$	$(1,1); (5/13,1); (3/7,3/7); (1,1/5)$
21	$SQ_1[21]$	36	$1 - 11$	$(1,1); (5/9,1); (7/11,7/11); (1,5/9)$
21	$NT_5[3,2,2,1,14]$	64	$5 - 28$	$(1,1); (1/3,1); (1,1/5)$
21	$NT_5[14,1,2,2,3]$	64	$5 - 28$	$(1,1); (1/5,1); (1,1/3)$
21	$SQ_7[4,2,1,7,1,2,4]$	16	$7 - 13$	$(1,1); (5/9,1); (7/11,7/11); (1,5/9)$
21	$NQ_8[2,2,3,1,4,2,1,7]$	12	$8 - 14$	$(1,1); (3/5,1); (7/11,7/11); (1,1/2)$
21	$NQ_8[7,1,2,4,1,3,2,2]$	12	$8 - 14$	$(1,1); (1/2,1); (7/11,7/11); (1,3/5)$
21	$NQ_{10}[2,\ldots,2,3]$	22	$10 - 21$	$(1,1); (1/2,1); (5/7,3/7); (1,5/13)$
21	$NQ_{10}[3,2,\ldots,2]$	22	$10 - 21$	$(1,1); (5/13,1); (3/7,5/7); (1,1/2)$
24	$SQ_9[6,1,3,1,6,1,3,1,6]$	79	$9 - 26$	$(1,1); (5/13,1); (1/2,1/2); (1,5/13)$
24	$SHV_9[2,2,3,1,5,1,3,2,2]$	161	$9 - 33$	$(1,1); (1/5,1); (5/13,9/13); (2/3,2/3); (9/13,5/13); (1,1/5)$
24	$SH_{11}[4,1,4,1,4,1,4,1,4,1,4]$	94	$11 - 27$	$(1,1); (7/19,1); (17/43,29/43); (1/2,1/2); (29/43,17/43); (1,7/19)$
27	$SQ_1[27]$	36	$1 - 11$	$(1,1); (7/11,1); (9/13,9/13); (1,7/11)$
27	$NQ_6[10,1,2,3,1,6]$	124	$6 - 37$	$(1,1); (1/5,1); (11/19,10/19); (1,1/2)$
27	$NQ_6[6,1,3,2,1,10]$	124	$6 - 37$	$(1,1); (1/2,1); (10/19,11/19); (1,1/5)$
27	$NQ_8[2,3,2,1,8,1,2,4]$	32	$8 - 23$	$(1,1); (5/13,1); (7/15,11/15); (1,7/11)$
27	$NQ_8[4,2,1,8,1,2,3,2]$	32	$8 - 23$	$(1,1); (7/11,1); (11/15,7/15); (1,5/13)$
…	…	…	…	…

References

[1] E. Alkan, A. H. Ledoan, A. Zaharescu, A parity problem on the free path length of a billiard in the unit square with pockets, preprint.

[2] F. P. Boca, C. Cobeli, A. Zaharescu, On the distribution of the Farey sequence with odd denominators, *Michigan Math. J.*, **51** (2003), 557–573.

[3] F. P. Boca, R. N. Gologan, A. Zaharescu, The average length of a trajectory in a certain billiard in a flat two-torus, *New York J. Math.* **9** (2003), 303–330.

[4] F. P. Boca, R. N. Gologan, A. Zaharescu, The statistics of the trajectory of a certain billiard in a flat two-torus, *Commun. Math. Phys.* **240** (2003), no. 1–2, 53–73.

[5] F. P. Boca, R. N. Gologan, A. Zaharescu, Sur le modéle du gaz de Lorentz périodique, *An. Univ. Craiova Ser. Mat. Inform.* **30** (2003), no. 1, 63–70.

[6] F. P. Boca and A. Zaharescu, Farey fractions and two-dimentional tori, in *Noncommutative Geometry and Number Theory* (C. Consani, M. Marcolli, eds.), Aspects of Mathematics E37, Vieweg Verlag, Wiesbaden, 2006, 57–77.

[7] J. Bourgain, F. Golse, and B. Wennberg, On the distribution of free path lengths for the periodic Lorentz gas, *Commun. Math. Phys.* **190** (1998), 491–508.

[8] L. A. Bunimovich, Billiards and other hyperbolic systems, in Ya G. Sinaie et al., eds., *Dynamical Systems, Ergodic Theory and Applications*, Encyclopaedia of Math. Sci. **100**, 2nd ed., Springer-Verlag, Berlin, 2000, pp. 192–233.

[9] C. Cobeli, A. Zaharescu, The Haros-Farey sequence at two hundred years, *Acta Univ. Apulensis Math. Inform.* **5** (2003), 1–38.

[10] C. Cobeli, A. Iordache, A. Zaharescu, The relative size of consecutive odd denominators in Farey series, *Integers*, **3**, A7, (2003), 14 pp. (electronic).

[11] C. Cobeli, A. Zaharescu, A density theorem on even Farey fractions, preprint.

[12] C. Cobeli, A. Zaharescu, On the small neighbor denominators of the Farey series with denominators in arithmetic progression, preprint.

[13] A. Haynes, A note on Farey fractions with odd denominators, *J. Number Theory* **98** (2003), 89–104.

[14] A. Haynes, The distribution of special subsets of the Farey sequence, *J. Number Theory* **107** (2004), 95–104.

[15] R. R. Hall and P. Shiu, The index of a Farey sequence, *Michigan Math. J.* **51** (2003), 209–223.

2000 *Mathematics Subject Classification*: Primary 11B57.
Keywords: Farey fractions, arithmetic progressions, congruence constraints.

Received September 15 2004; revised version received May 20 2005; July 20 2006. Published in *Journal of Integer Sequences*, July 20 2006.

Return to Journal of Integer Sequences home page.

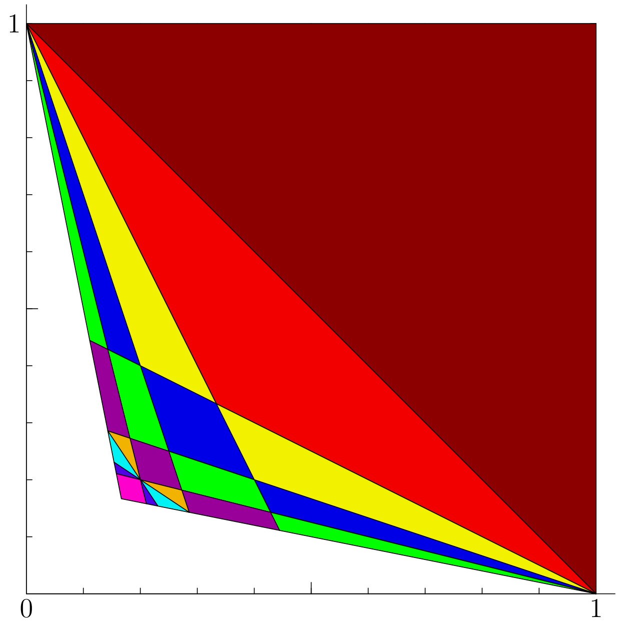

Fig. 2: Kernel=1; $\mathfrak{d} = 5$, $\mathfrak{c} = 1, 2, 3$ or 4.
The mosaic $SQ_0[\cdot]$.

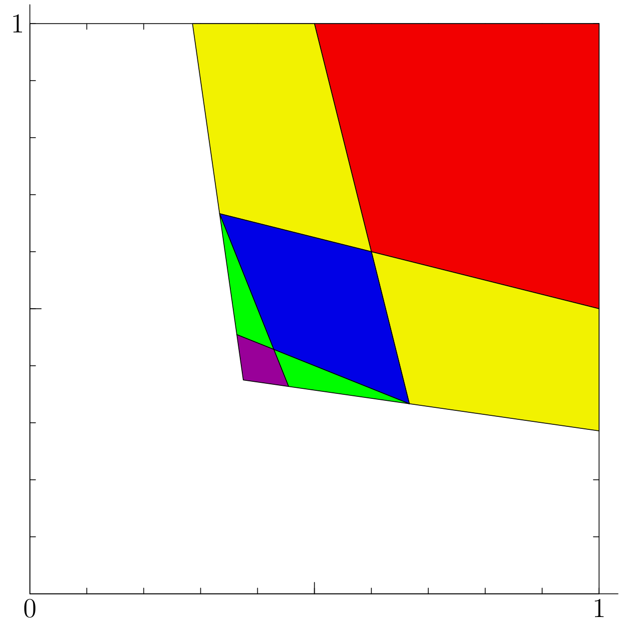

Fig. 3: Kernel=3; $\mathfrak{d} = 5$, $\mathfrak{c} = 1, 2, 3$ or 4.
The mosaic $SQ_1[3]$.

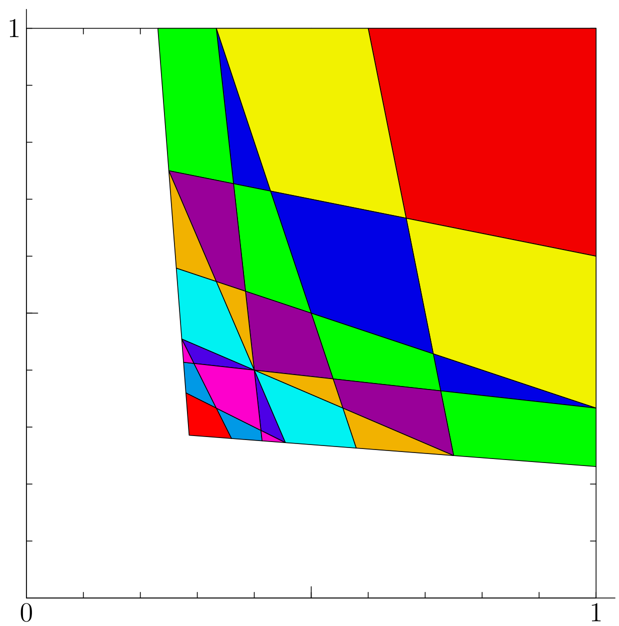

Fig. 4: Kernel=4; $\mathfrak{d} = 5$, $\mathfrak{c} = 1, 2, 3$ or 4.
The mosaic $SQ_1[4]$.

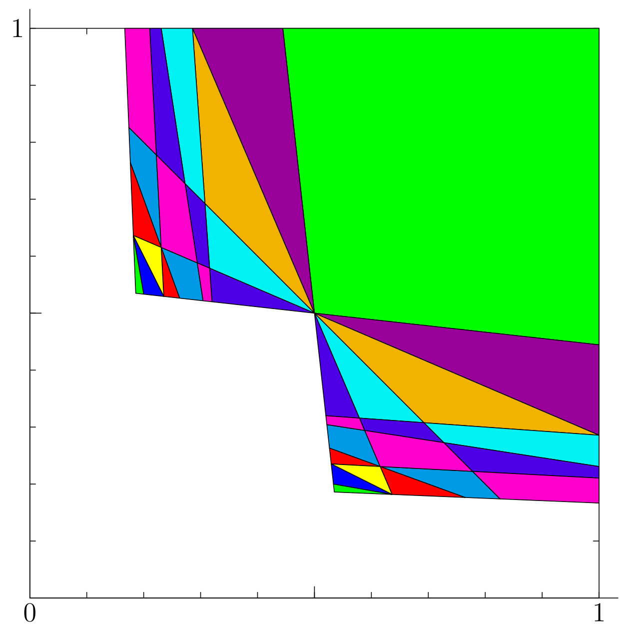

Fig. 5: Kernel=5; $\mathfrak{d} = 5$, $\mathfrak{c} = 1, 2, 3$ or 4.
The mosaic $SHV_4[2, 2, 2, 2]$.

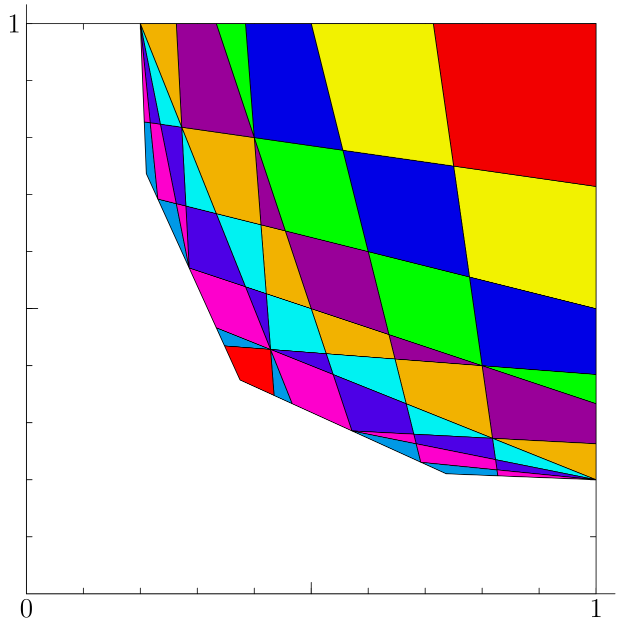

Fig. 6: Kernel=6; $\mathfrak{d} = 5$, $\mathfrak{c} = 1, 2, 3$ or 4.
The mosaic $SH_1[6]$.

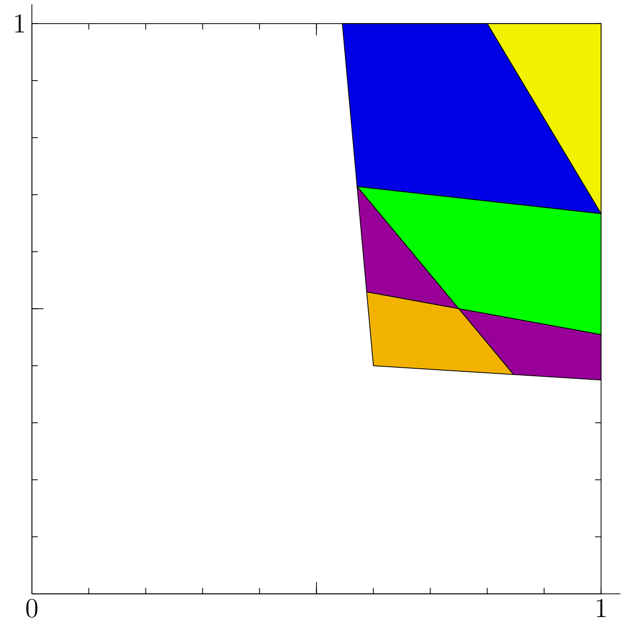

Fig. 7: Kernel=7; $\mathfrak{d} = 5$, $\mathfrak{c} = 1, 2, 3$ or 4.
The mosaic $NQ_2[2, 4]$.

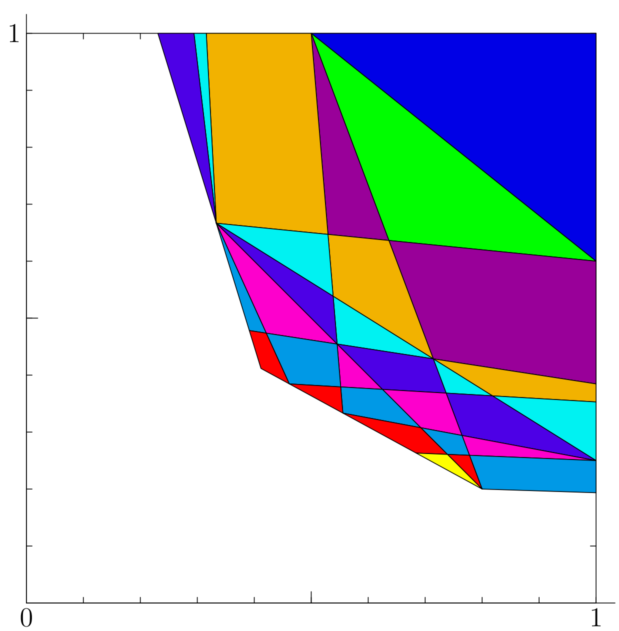

Fig. 8: Kernel=7; $\mathfrak{d} = 5$, $\mathfrak{c} = 1, 2, 3$ or 4.
The mosaic $NP_3[2, 2, 3]$.

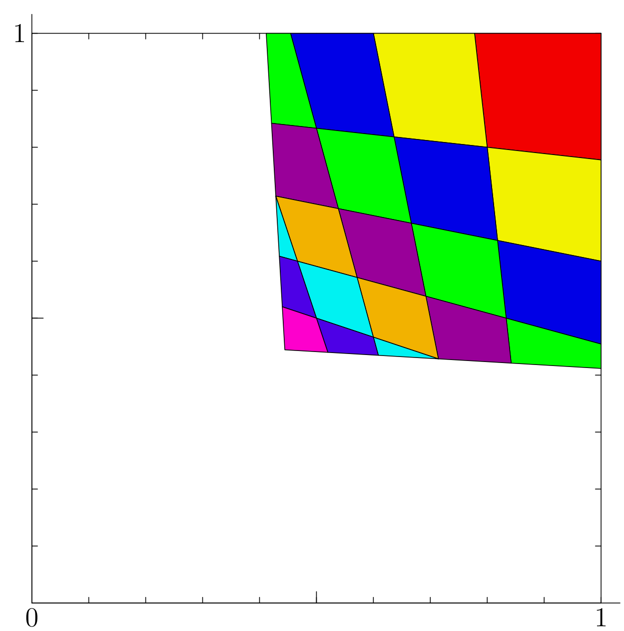

Fig. 9: Kernel=8; $\mathfrak{d} = 5$, $\mathfrak{c} = 1, 2, 3$ or 4.
The mosaic $SQ_1[8]$.

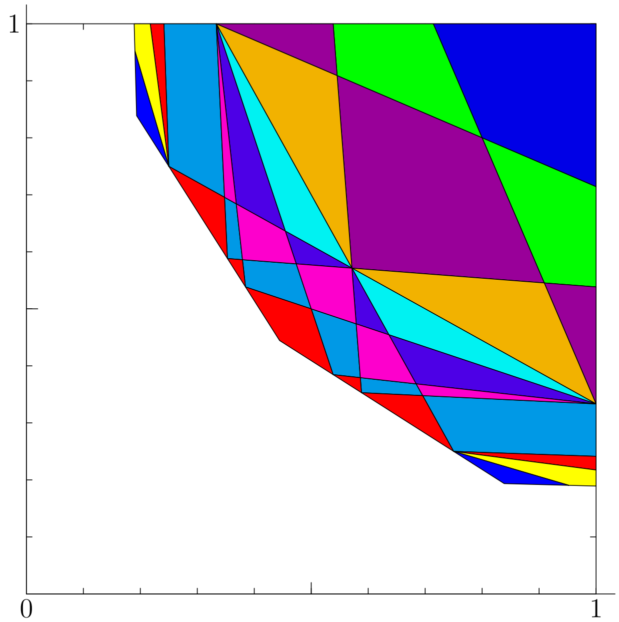

Fig. 10: Kernel=8; $\mathfrak{d} = 5$, $\mathfrak{c} = 1, 2, 3$ or 4.
The mosaic $SH_3[2, 3, 2]$.

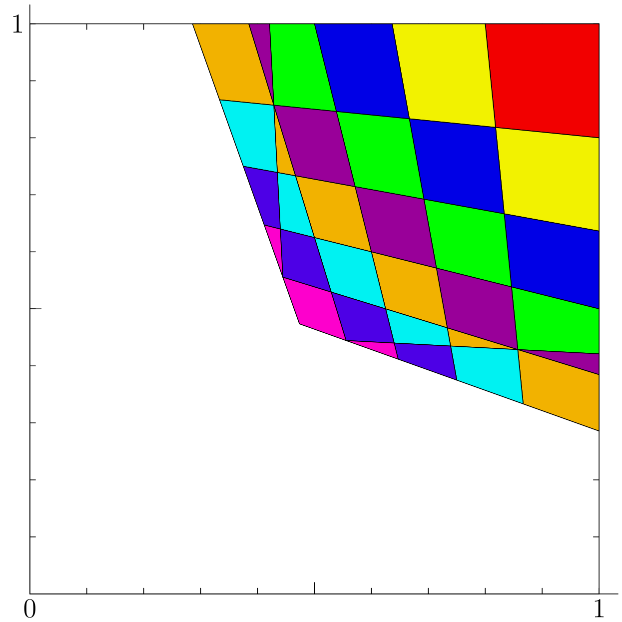

Fig. 11: Kernel=9; $\mathfrak{d} = 5$, $\mathfrak{c} = 1, 2, 3$ or 4.
The mosaic $SQ_1[9]$.

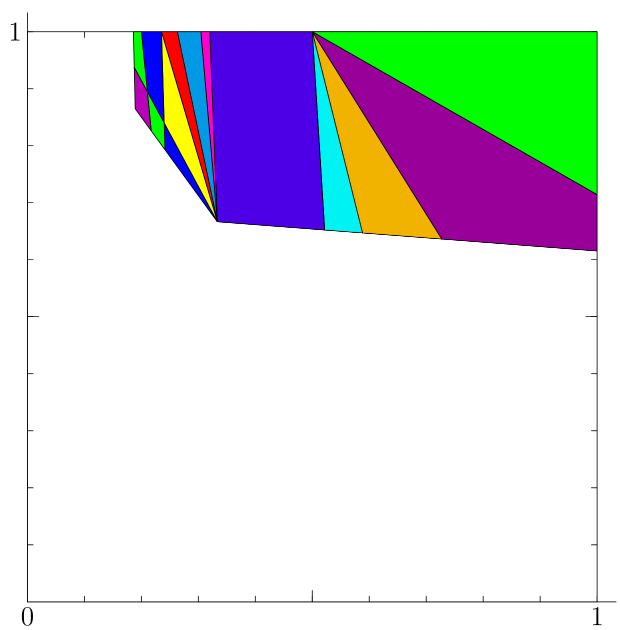

Fig. 12: Kernel=9; $\mathfrak{d} = 5$, $\mathfrak{c} = 1, 2, 3$ or 4.
The mosaic $NP_4[2, 2, 2, 3]$.

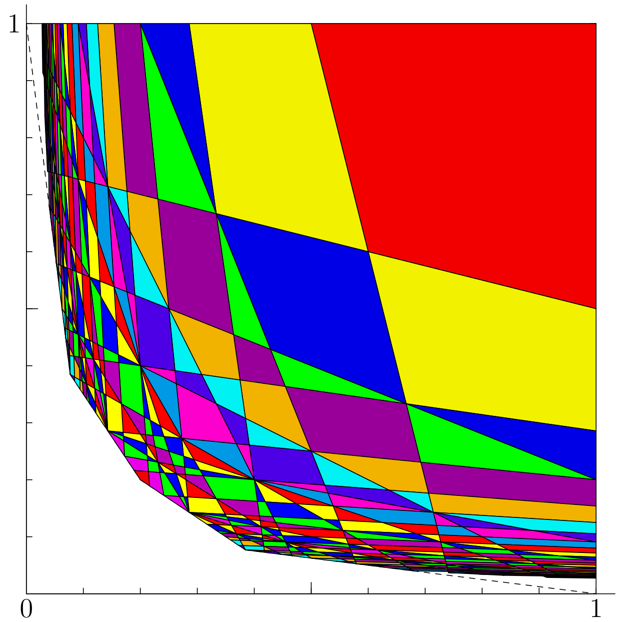

Fig. 13: Kernel=3; $\mathfrak{d} = 12$, $\mathfrak{c} = 3$.
The mosaic $SH_1[3]$.

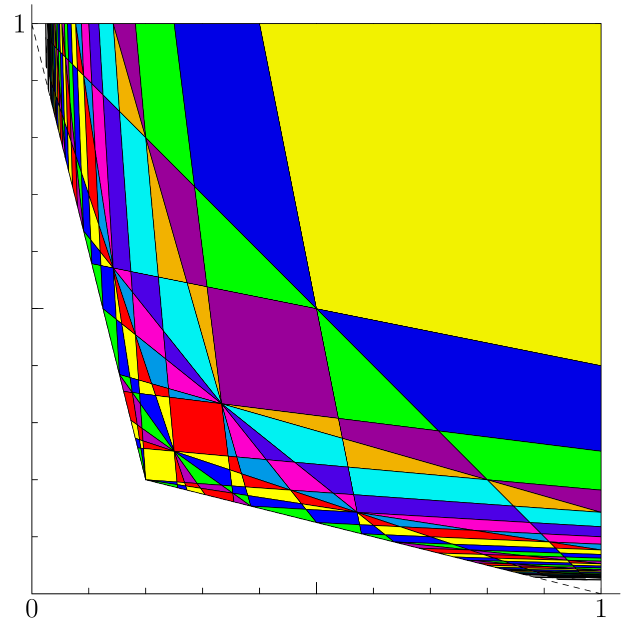

Fig. 14: Kernel=3; $\mathfrak{d} = 12$, $\mathfrak{c} = 3$.
The mosaic $SQ_2[2, 2]$.

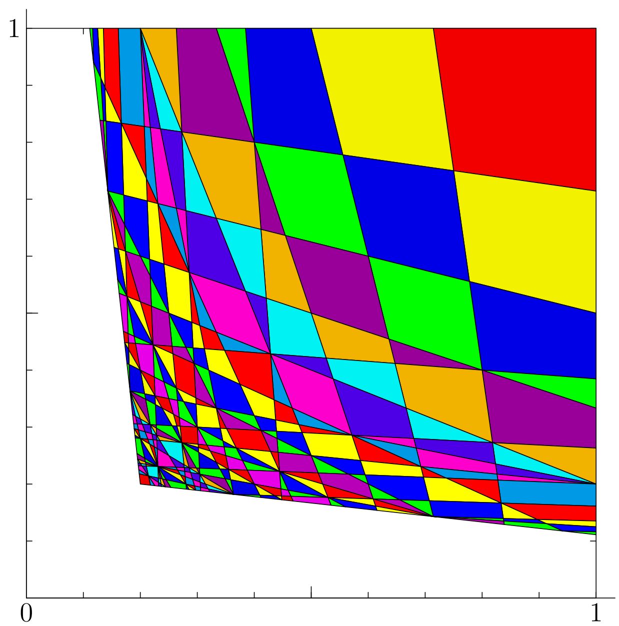

Fig. 15: Kernel=6; $\mathfrak{d} = 12$, $\mathfrak{c} = 3$.
The mosaic $SQ_1[6]$.

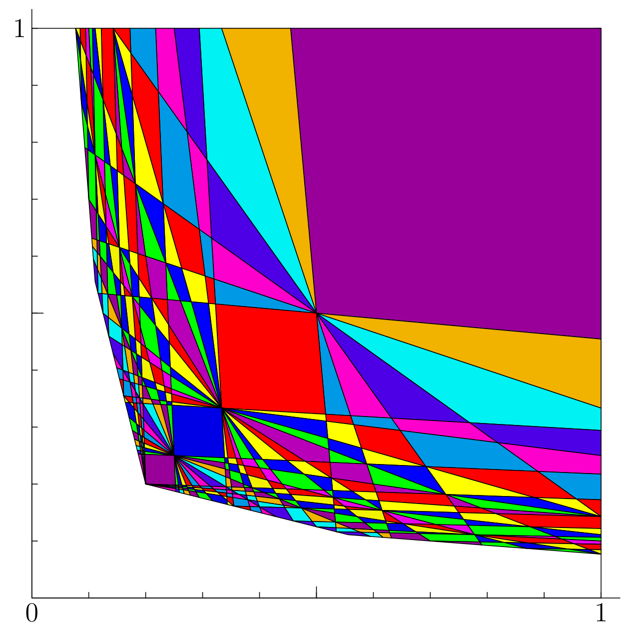

Fig. 16: Kernel=6; $\mathfrak{d} = 12$, $\mathfrak{c} = 3$.
The mosaic $SQ_5[2, 2, 2, 2, 2]$.

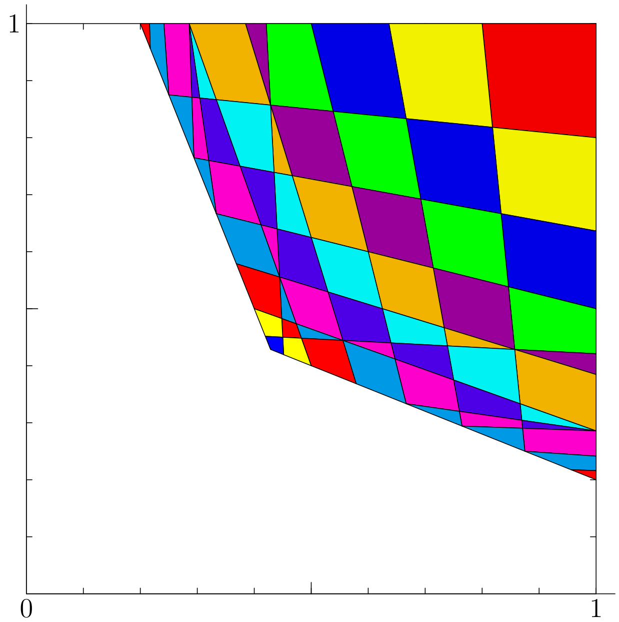

Fig. 17: Kernel=9; $\mathfrak{d} = 12$, $\mathfrak{c} = 3$.
The mosaic $SQ_1[9]$.

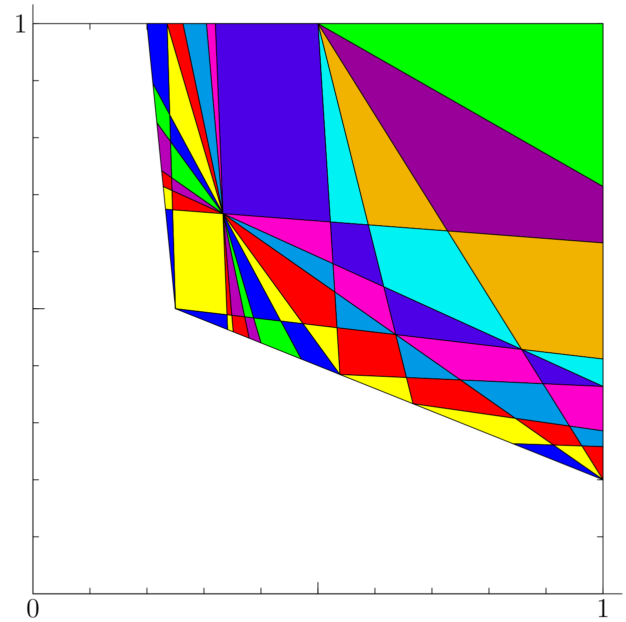

Fig. 18: Kernel=9; $\mathfrak{d} = 12$, $\mathfrak{c} = 3$.
The mosaic $NQ_4[2, 2, 2, 3]$.

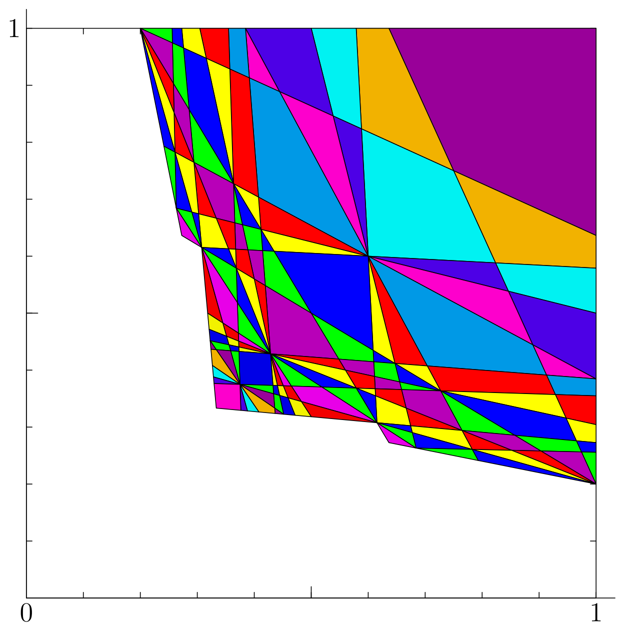

Fig. 19: Kernel=12; $\mathfrak{d} = 12$, $\mathfrak{c} = 3$.
The mosaic $SO_5[3, 1, 6, 1, 3]$.

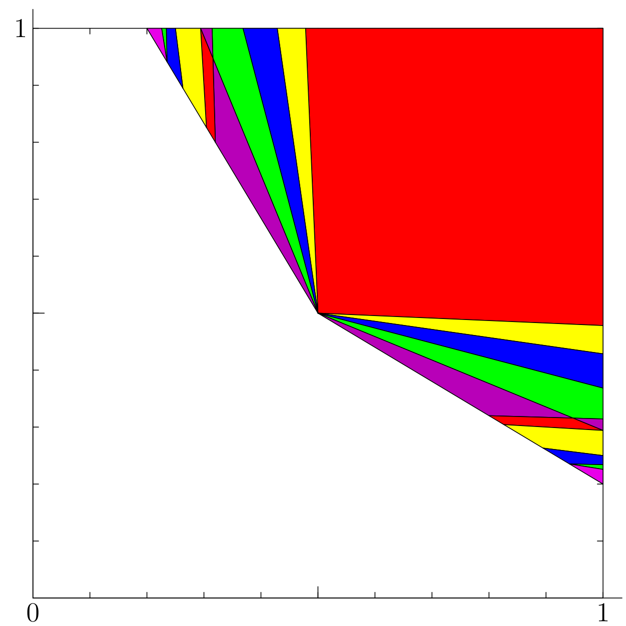

Fig. 20: Kernel=12; $\mathfrak{d} = 12$, $\mathfrak{c} = 3$.
The mosaic $SQ_{11}[2, \ldots, 2]$.

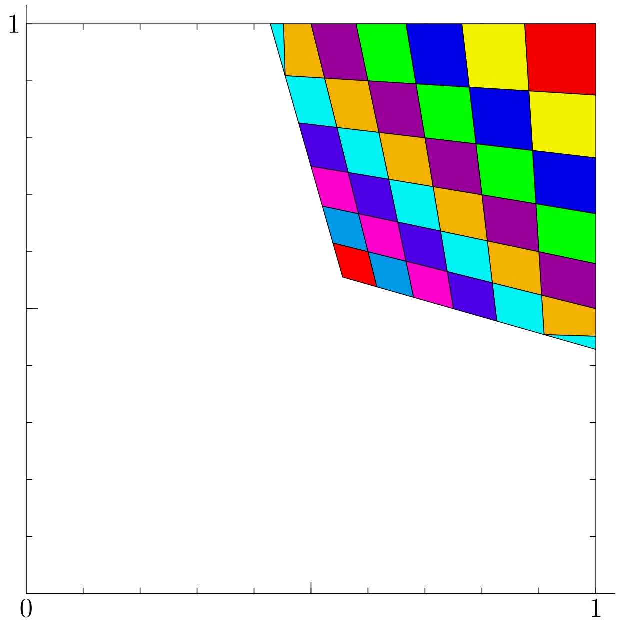

Fig. 21: Kernel=15; $\mathfrak{d} = 12$, $\mathfrak{c} = 3$.
The mosaic $SQ_1[15]$.

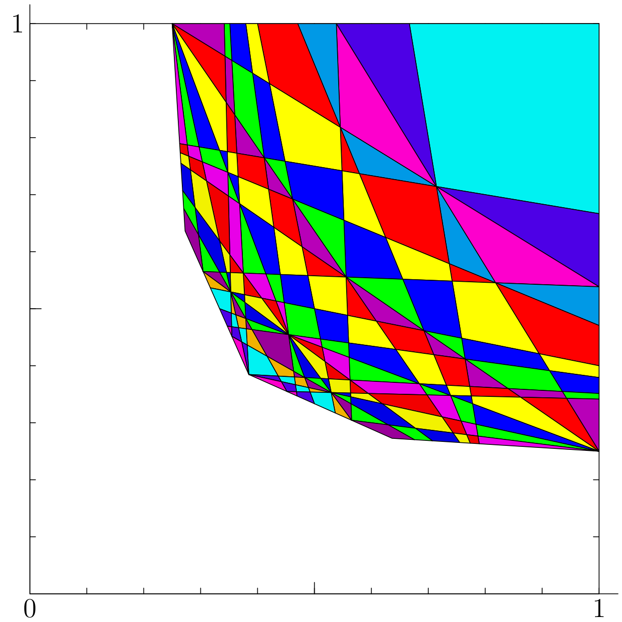

Fig. 22: Kernel=15; $\mathfrak{d} = 12$, $\mathfrak{c} = 3$.
The mosaic $SH_7[2, 3, 1, 5, 1, 3, 2]$.

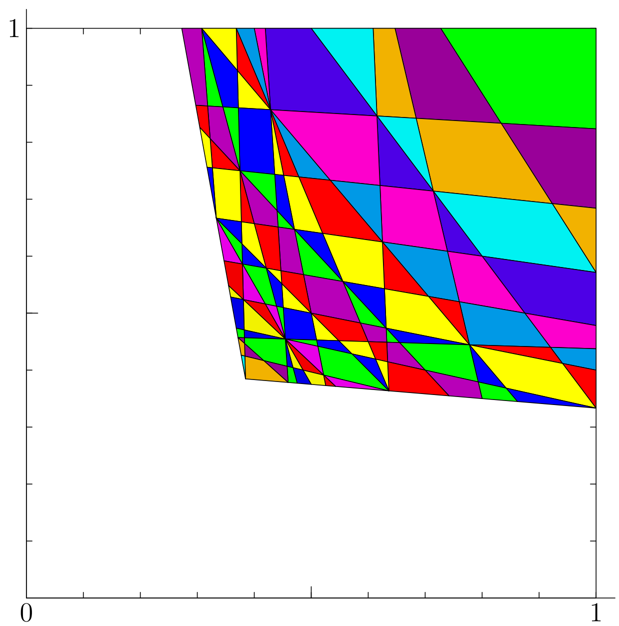

Fig. 23: Kernel=15; $\mathfrak{d} = 12$, $\mathfrak{c} = 3$.
The mosaic $NQ_4[3, 2, 1, 10]$.

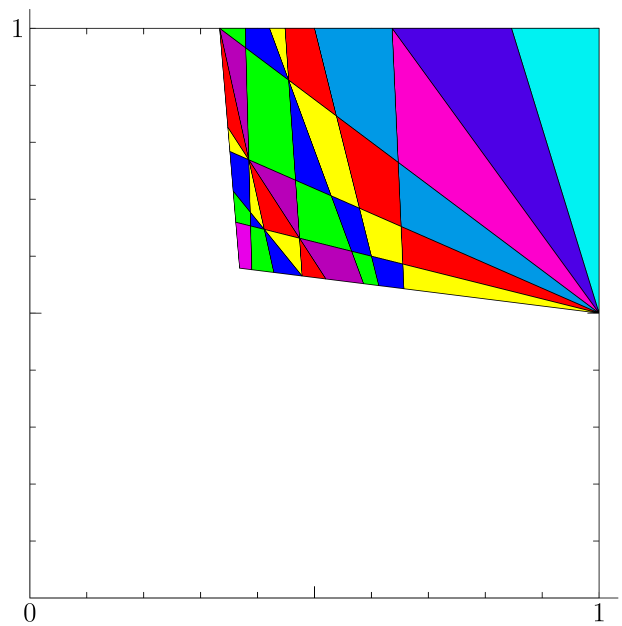

Fig. 24: Kernel=15; $\mathfrak{d} = 12$, $\mathfrak{c} = 3$.
The mosaic $NQ_7[3, 2, 2, 2, 2, 2, 2]$.

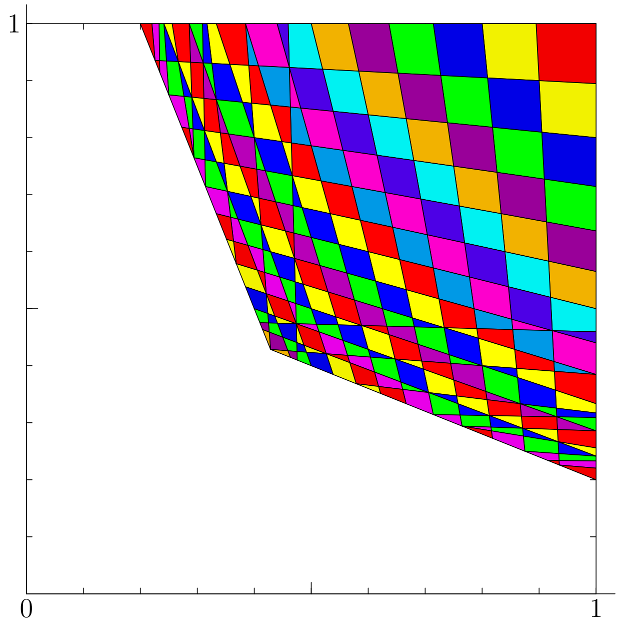

Fig. 25: Kernel=18; $\mathfrak{d} = 12$, $\mathfrak{c} = 3$.
The mosaic $SQ_1[18]$.

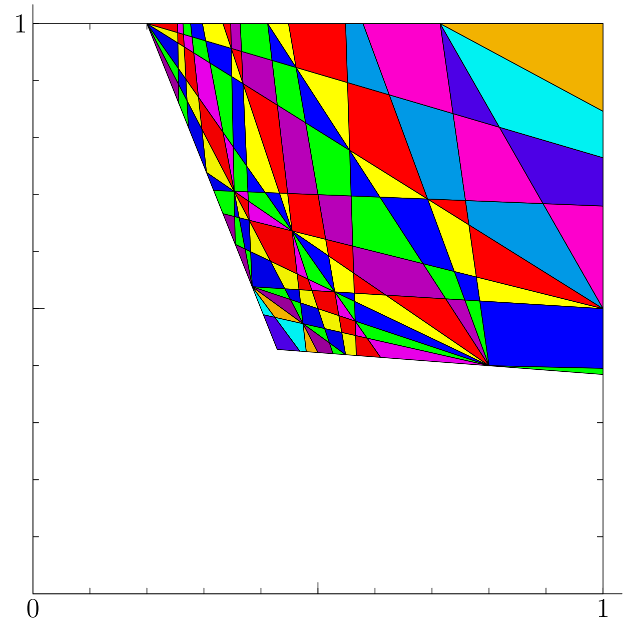

Fig. 26: Kernel=18; $\mathfrak{d} = 12$, $\mathfrak{c} = 3$.
The mosaic $NQ_6[2, 3, 1, 5, 1, 4]$.

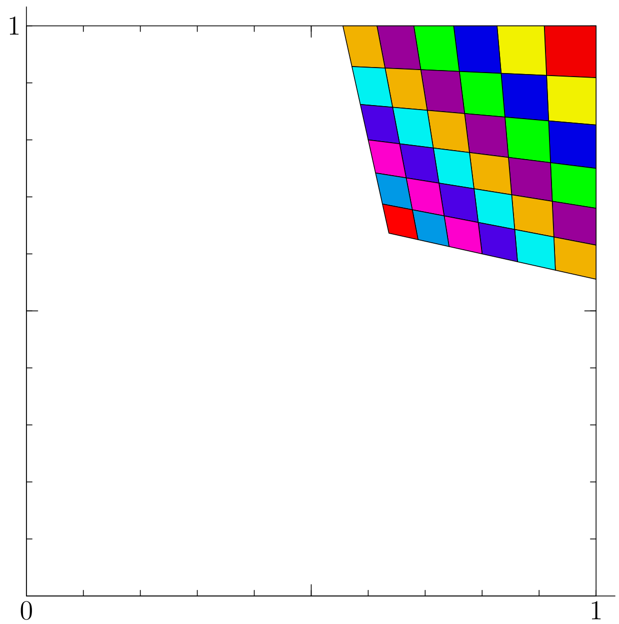

Fig. 27: Kernel=21; $\mathfrak{d} = 12$, $\mathfrak{c} = 3$.
The mosaic $SQ_1[21]$.

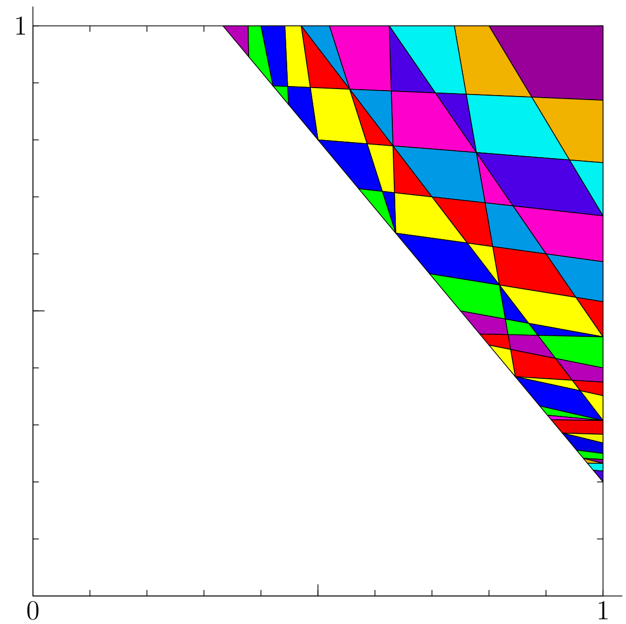

Fig. 28: Kernel=21; $\mathfrak{d} = 12$, $\mathfrak{c} = 3$.
The mosaic $NT_5[3, 2, 2, 1, 14]$.

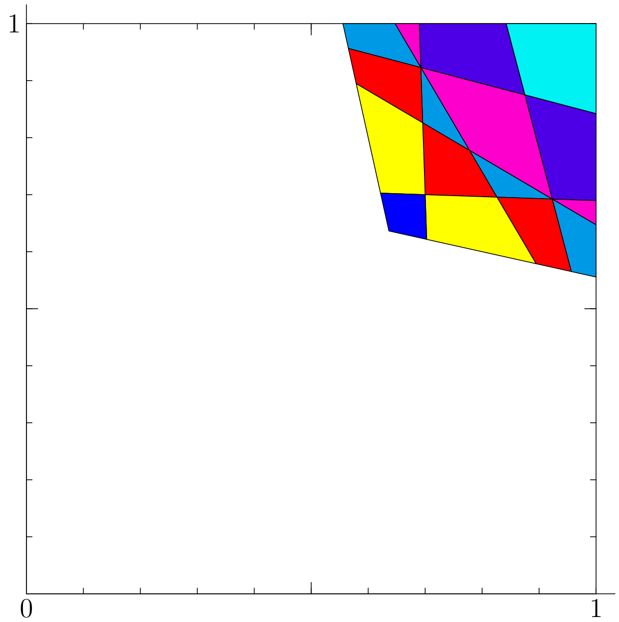

Fig. 29: Kernel=21; $\mathfrak{d} = 12$, $\mathfrak{c} = 3$.
The mosaic $SQ_7[4, 2, 1, 7, 1, 2, 4]$.

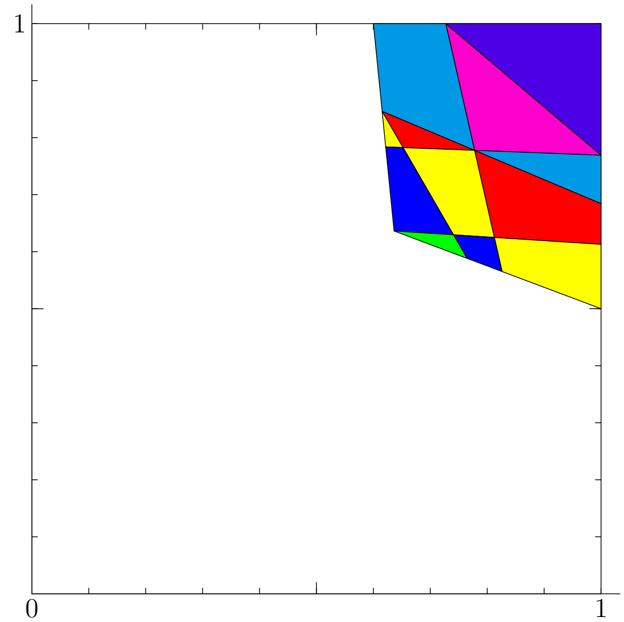

Fig. 30: Kernel=21; $\mathfrak{d} = 12$, $\mathfrak{c} = 3$.
The mosaic $NQ_8[2, 2, 3, 1, 4, 2, 1, 7]$.

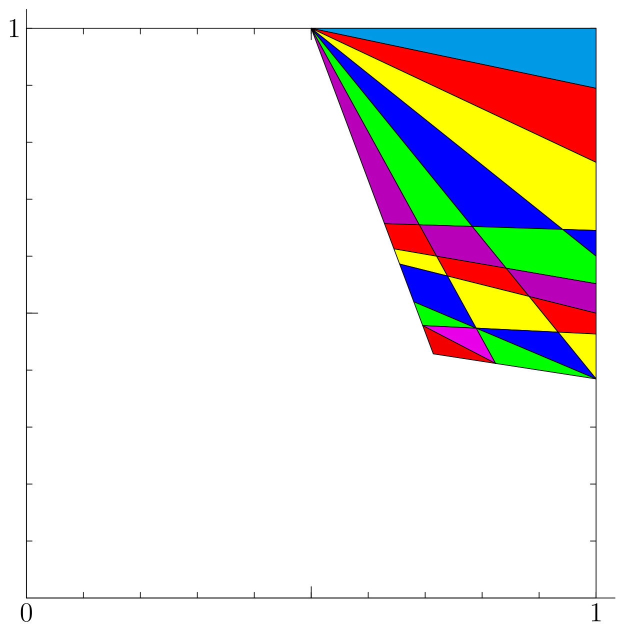

Fig. 31: Kernel=21; $\mathfrak{d} = 12$, $\mathfrak{c} = 3$.
The mosaic $NQ_{10}[2, \ldots, 2, 3]$.

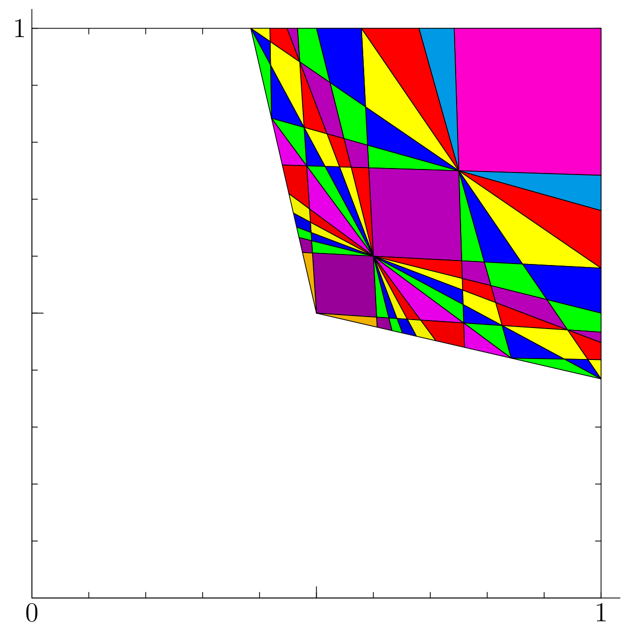

Fig. 32: Kernel=24; $\mathfrak{d} = 12$, $\mathfrak{c} = 3$.
$SQ_9[6, 1, 3, 1, 6, 1, 3, 1, 6]$.

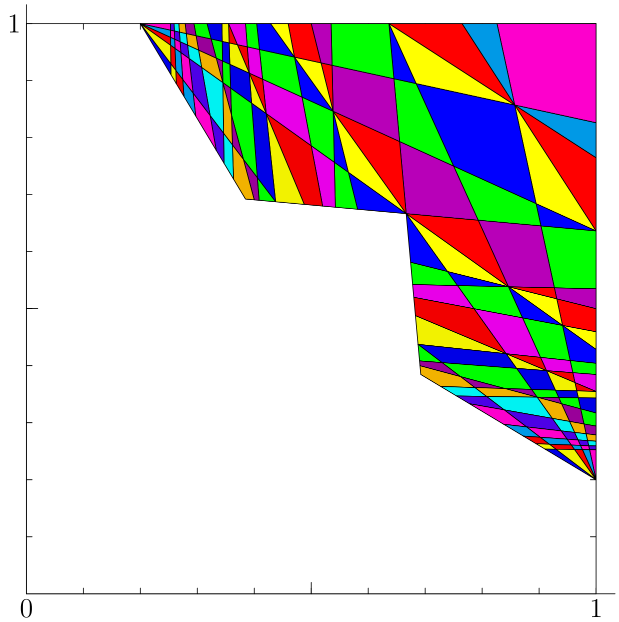

Fig. 33: Kernel=24; $\mathfrak{d} = 12$, $\mathfrak{c} = 3$.
$SHV_9[2, 2, 3, 1, 5, 1, 3, 2, 2]$.

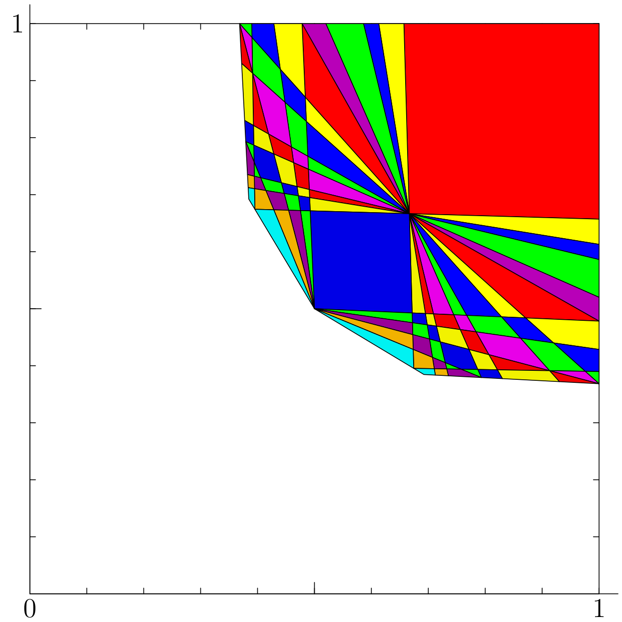

Fig. 34: Kernel=24; $\mathfrak{d} = 12$, $\mathfrak{c} = 3$.
$SH_{11}[4, 1, 4, 1, 4, 1, 4, 1, 4, 1, 4]$

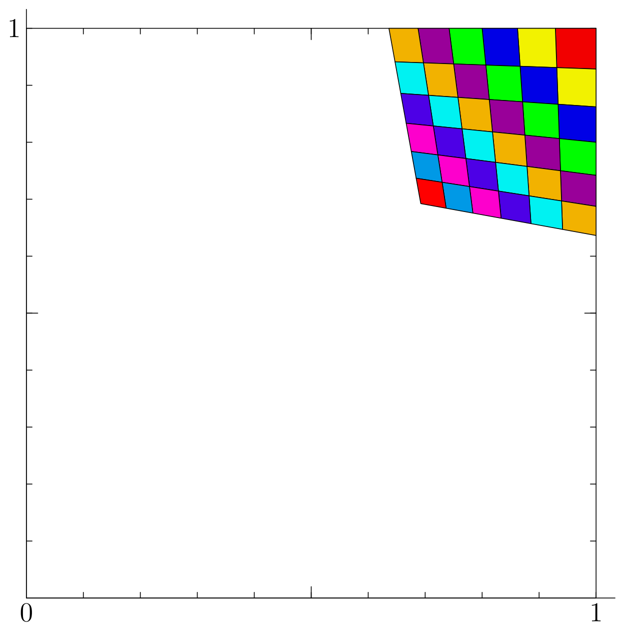

Fig. 35: Kernel=27; $\mathfrak{d} = 12$, $\mathfrak{c} = 3$.
The mosaic $SQ_1[27]$.

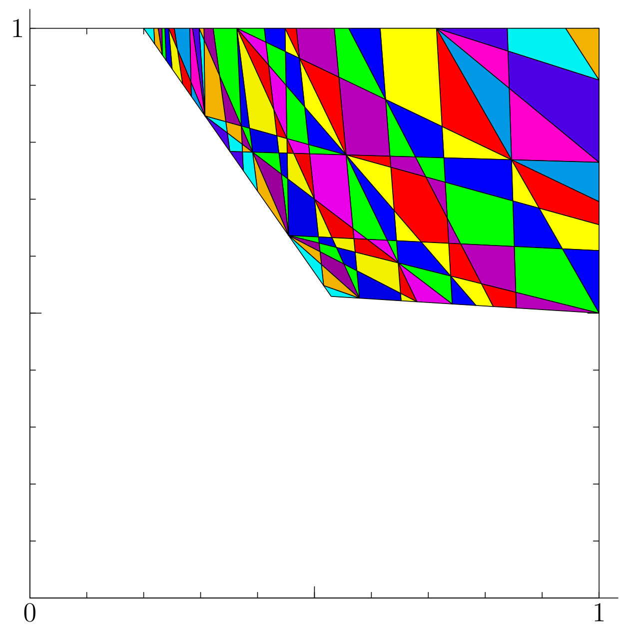

Fig. 36: Kernel=27; $\mathfrak{d} = 12$, $\mathfrak{c} = 3$.
The mosaic $NQ_6[10, 1, 2, 3, 1, 6]$.

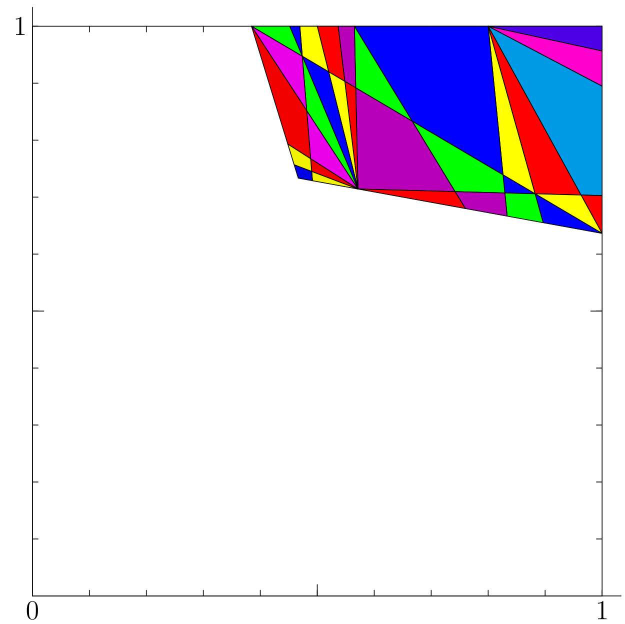

Fig. 37: Kernel=27; $\mathfrak{d} = 12$, $\mathfrak{c} = 3$.
The mosaic $NQ_8[2, 3, 2, 1, 8, 1, 2, 4]$.